ROLE OF ACTIN AND MYOSIN IN THE AMOEBOID MOVEMENT OF DICTYOSTELIUM

Shigehiko Yumura

A Doctoral Thesis submitted by S. Yumura
to Faculty of Science, Osaka University

CONTENTS

Abbreviations used in this thesis

BSS: Bonner's salt solution

cAMP: adenosine 3',5'-cyclic monophosphate

DM-2: monoclonal antibody against *Dictyostelium* myosin

DMSO: dimethyl sulfoxide

FITC: fluorescein isothiocyanate

MTOC: microtubule organizing center

SDS PAGE: sodium dodecyl sulfate polyacrylamide gel electrophoresis

PBS: phosphate-buffered saline

I. SUMMARY

I studied the total cytoskeleton of Dictyostelium amoebae, which is composed of microtubule and microfilament systems, to clarify their distributions and physiological functions. This thesis is organized with three parts of documentations.

In the first part, the microtubule system in Dictyostelium amoebae is described. The system is composed of about 30 microtubules radiating from the MTOC associating with the nucleus. The roles of the cytoplasmic microtubules in Dictyostelium amoebae have been thought to be the retention of cell shape, intracellular transport and the establishment of cellular polarity. The third function was specifically investigated in this study. First, the cytoplasmic microtubules and MTOC were observed in the aggregating cells using improved indirect immunofluorescence ("agar-overlay" technique). The results indicated that the MTOC was located in the anterior side of the nucleus at a significant probability. Second, the location of MTOC was investigated in living cells. The MTOC was located in the middle of the cytoplasm, suggesting that it might function to fix the nucleus in the center of the locomoting cells.

Second, the microfilament system of Dictyostelium amoebae was localized mainly at the cortical region. The cellular motile activity drastically changes during the early development. The amount of Triton X-100 insoluble ghost turned out to change corresponding to the motile activity. This observation indicated

that the enhansment of the motile activities was dependent on the increment of the motile machinery of the cells.The distribution of actin and myosin during the early development was studied using polyclonal anti-actin and newly obtained monoclonal anti-Dictyostelium myosin antibodies. The actin staining was diffusible in the cytoplasm while myosin was localized at the cortical region in the vegetative cells. When the amoebae were compelled to start development, both actin and myosin stainings were localized at the cortical region of non-migrating round cells. In actively migrating cells displaying the morphorogical polarity with a pseudopode at the front end and a tail at the posterior end, both actin and myosin stainings were localized at the posterior cortex whereas only actin staining was localized at the anterior pseudopode. These observations implied that the motive force for the amoeboid movement is located at the posterior cortex.

Third, the improvement of the immunofluorescent fixation made it possible to visualize the myosin rods in Dictyostelium amoebae. The dimension of these rods was similar to that of reconstituted thick filaments. The distribution of these rods was investigated during the early deveolopment. They were localized at the cortical region in vegetative cells. They appeared in the endoplasm as well as in the cortex. In developing cells, in dividing cells, they were aligned in parallel with each other around the cleavage furrow. Strikingly, cAMP, a chemoattractant of Dictyostelium amoebae, induced a rapid and reversible changes in the distribution of the thick filaments: they disappeared from the endoplasm and accumulated in the cortex.

This change was suggested to be correlated with the contraction of the cell or the extention of pseudopode in response to the chemotactic stimulation. Folic acid, a chemoattractant of vegetative cells, also induced a rapid change in the distribution of the thick filaments. The study using the calcium ionophore implicated that the increase in intracellular calcium triggered the changes in the distribution of myosin rods.

II. INTRODUCTION

Since the cellular slime mold was first discovered by O. Brefeld in 1869, many researches have been performed on their unique life cycle and development. The life cycle of Dictyostelium is divided into two distinct phases: the vegetative phase, during which the organism feeds and divides as long as food bacteria are present and; the developmental phase, which is triggered by the exhaustion of the bacteria, after which cells aggregate to the center, forming a multicellular mass and differentiate into a fruiting body.

During the early developmental phase, the aggregation center release a pulsatile chemotactic signal(101) which is relayed by responding cells. The signal have been demonstrated to be 3',5'-cyclic AMP(10). Also in a multicellular mass cAMP is released from the frontal tip and thought to play a crucial role in determining of developmental fate of the cells.

During the life cycle of Dictyostelium, very active cell movement is observed. Samuel (86) demonstrated that the rate of cell movement drastically changed during the life cycle. During 2 hrs after the harvest, the rate increases abruptly, then it decreases untill the second increase at the aggregation phase.

Many aspects of cell motility in eucaryotic cells are thought to share some common molecular basises. These molecules are organized forming supramolecular structure termed as cytoskeleton. Cytoskeleton is basically composed of three filament systems: microfilament, microtubule and intermediate

filament. Processes, such as amoeboid movement, cytoplasmic streaming, cell division, endo- and exocytosis and accumulation of receptors on the cell membrane are all thought to involve the microfilament-based mechanism. Microtubule system is thought to play important roles in mitosis, intracellular transport and cell movement. Intermediate filament system is believed to support the cytoplasmic matrix (but have not been described in Dictyostelium). This thesis documents the organization of microtubule and microfilament systems in Dictyostelium.

In Dictyostelium, microtubule system has been studied by electron microscopy and immunofluorescent microscopy. Spindle microtubules in mitotic cells were well observed by Roos (81). However, tubulin, the major molecular component of microtubule, has not been purified by conventional method and its biochemical nature have not been elucidated (108). The approach using microtubule inhibitors revealed that Dictyostelium microtubules work in not only maintaining cell shape but also in normal development (51). This thesis describes in more detail the distribution of the cytoplasmic microtubules in interphase cells by indirect immunofluorescence supporting the Albrecht-Buehler's hyposesis(3) that MTOC may play an important role in the determination of the direction of cell locomotion.

The study of the microfilament system in Dictyostelium has been performed mainly by ultrastructual studies (26) or by the analysis of the properties of actin rich cell extract (97,98). This organism is a good material for studying cell motility because it migrates by amoeboid movement, one of the most

conservative mechanism of cell motility. Biochemical and electron microscopic studies have revealed the significant concomitance of actin, myosin, and their associated proteins in cellular motile events of Dictyostelium. The solation-contraction coupling hypothesis of Hellewell and Taylor (42) suggests a structural requirement of local breakdown of the gel for contraction in the motile extract of Dictyostelium. However, the structural organization of the contractile components in intact cells has not been fully clarified. This thesis describe the importance of the cortical microfilaments in the motile activity of Dictyostelium using a unique microfilament inhibitor: dimethyl sulfoxide (DMSO).

Initial immunofluorescence using anti-actin showed that the vegetative amoebae were stained uniformly whereas actively migrating cells were stained strongly at the leading edge (27). Recently, Bazari and Clarke demonstrated that calmodulin and myosin are localized in the peripheral region (6,7). Condeelis et al. (20) and Brier et al. (13), using conventional immunofluorescence, found that 120 K and 95 K actin-binding proteins are also localized at the cell periphery. However, partially because of the round shape and small size of Dictyostelium amoebae, no detailed information on the spacial organization of cytoskeletal components has been provided by conventional immunofluorescence. The present study documents the localization of actin and myosin in various developmental stages of amoebae revealed by the improved agar-overlay technique using rabbit anti-actin and newly obtained monoclonal anti-Dictyostelium myosin antibodies. The agar-overlay technique

could preserve cellular structures during the fixation and prevent their disruption during sample preparation.

Interestingly, very specific myosin staining was observed at the posterior cortex of the migrating amoebae, whereas actin staining was localized in the anterior pseudopodes and the posterior cortex. This finding suggested that the motive force of amoeboid movement is generated the posterior cortex of migrating cells. The possible role of actin in the anterior pseudopode is discussed in relation to speculative coupling in the organization of cytoskeletal elements involved in the amoeboid movement.

The mode of *in situ* organization of myosin molecules has not been clarified not only in *Dictyostelium* but also other non-muscle cells (44). Myosin isolated from non-muscle cells can be induced to polymerize and form bipolar thick filaments *in vitro* as well as one from muscle cells by low ion stlength solution. Myosin in muscle cells, which exist as thick filaments *in situ*, is thought to form crossbridges and slide with thin filaments composed of actin. In *Dictyostelium* myosin was purified initially by Clark & Spudich (16) and shown to be regulated by phosphorylation of the heavy chain described by Kuzumarski & Spudich (53). Recently, Malchow et al. indicated the transient phosphorylation of myosin in responding cells to chemotactic stimulation (61).

This thesis documents the identification and localization of myosin rods and their dynamic translocation in response to exogeneously added cAMP in *Dictyostelium* amoebae. Some evidences

demonstrated that these rods represent the thick filaments of myosin. The presence and drastic alignment of the rods in the cortical region of vegetative cells were made visible by ameliorated immunofluorescence. During the mitotic phase, the cortical rods mostly disappeared and distinct fluorescence appeared at the cleavage furrow. After the cessation of growth, the myosin rods increased in number and numerous rods were also seen in the endoplasm. In polarized cells, the rods were specifically localized at the posterior cortex. On treatment with cAMP, very rapid transient translocation of the myosin was observed; instantaneous shedding of the endoplasmic myosin was followed by an increase in original distribution in a few minutes.

III. Materials and Methods

Cells: Dictyostelium mucoroides cells, strain Dm-7, were cultured by liquid shake culture in 17 mM Na/K-Sörensen's phosphate buffer (pH 6.5) with Escherichia coli (B/r) at 22 °C. Dictyostelium discoideum, strain NC-4, was grown with E. coli on nutrient agar and used for all the immunofluorescence. Dictyostelium discoideum, strain AX-2, was axenically cultured in HL-5 medium (17) for the purification of myosin. The cells were harvested at the logarithmic growth stage by centrifugation (300g, 1.5 min), washed and suspended in Bonner's salt solution (BSS) (10) containig 10 mM NaCl, 10mM KCl and 3mM $CaCl_2$. They were inoculated on 2 % agar plate and allowed to develop until the appropriate stages. On this condition aggregation begins 6 hours after a harvest.

Membrane Preparations: The membrane fraction was prepared according to Spudich (93), with slight modifications. Preaggregation cells were treated with 5% DMSO in BSS for 0 (control), 5, 15 and 30 min. Immediately after centrifugation, the cell pellet (1 ml) was frozen in liquid nitrogen. Five mililiters of cold buffer (preparation buffer: 30% [wt/wt] sucrose, 100 mM KCl, 5 mM EGTA, 1 mM dithiothreitol [DTT], 0.1mM phenylmethylsulfonyl fluoride [PMSF], and 0.1 mM p-tosyl-L-Lysine chloromethylketone hydrochrolide [TLCK] in 10 mM Tris-HCl, pH 7.6) was added to the frozen cells, and the cells were thawed at room temperature. This suspension contained plasma membrane ghosts of the disrupted cells, according to observations under a

phase-contrast microscope. After two cycles of centrifugation (12,000 g, 40 min), the pellet was suspended in 2 ml of the cold preparation buffer and layered on top of a sucrose stepwise gradient (2.5 ml of 35% [wt/wt], 2.5 ml of 45% [wt/wt], and 2.5 ml of 55% [wt/wt] in the buffer). After centrifugation (12,000 g, 3 h), the 35-45% boundary was collected and suspended in 1 ml of the preparation buffer. Usually, this suspension contained about 2 mg/ml of protein associated with the plasma membrane.

SDS PAGE: The purified membrane preparations were boiled in SDS-sample buffer (20 mM Tris-HCl[pH6.5], 2% SDS, 20% glycerol, 2% 2-mercaptoethanol, and 0.01% bromophenol blue) for a few min. SDS PAGE was performed on 5-15% linear gradient polyacrylamide slab gel containing 0.1% SDS according to Laemmli (55). The densitometory was done with the gels stained with Coomassie Brillant Blue R at 550 nm using a Gelman model DCD-16 densitometer. Protein concentrations were estimated by the method of Lowry et al. (56) after acid precipitation (9).

Two-dimensional Gel Electrophoresis: The membrane preparations were solubilized by boiling for 2 min in 1% SDS and 5% 2-mercaptoethanol, and then urea and ampholine (LKB, pH3.5-10) and NP-40 were added to make 8.5M, 1.6% and 8% (5) in concentrations, respectively. The isoelectric focusing electrophoresis (first dimension) was done using glass tubes (0.15 mm in diameter, 16 cm in length) according to O'Farrel (75). The first dimension gels were equilibrated in the SDS-sample buffer, and the second dimension was done in 10% polyacrylamide slab gels and stained

with Coomassie Brilliant Blue R.

Electron microscopy: The cells were allowed to spread on Thermanox plastic cover slips (Lux Scientific Corporation, Newbury Park, CA) at a density of 1-2 X 10^6 cells/ml for 20 min at 20 °C. Then the cells were treated with DMSO for various periods and fixed with a mixture of 1% paraformaldehyde and 1.25% glutaraldehyde in 24 mM cacodylate buffer (pH 7.2) for 1 h. After postfixation with 1% OsO_4 in the buffer for 1 h, they were dehydrated through an ethanol series. For the SEM preparations, the samples were extracted with isoamylacetate and dried at critical point, then the gold-coated samples were observed under a Hitachi S-430 scanning electron microscope.

For the TEM preparations, the samples were embedded in Spurr's resin (Polyscience, Inc., Warrington, PA), and thin sections were observed under a JEM 100-C electron microscope after staining with uranyl acetate and lead citrate.

Derivation of Hibridomas: Dictyostelium myosin was purified according to methods of Clark and Spudich (16) and Mockrin and Spudich (71). Four 5-week-old mice were intraperitoneally injected with 100 μg of myosin in Freund's complete adjuvant. Two weeks later, a booster of 100 μg of myosin mixed with incomplete adjuvant was given intraperitoneally. One week later, the antibody activity was examined by enzyme-linked immunosorbent assay (ELIZA) (28) and all the mice gave positive results. Four weeks after the primary immunization, 200 μg of myosin in PBS [138 mM NaCl, 2.7 mM KCl, 8 mM Na/K-phosphate buffer (pH 7.2)]

was injected intraperitoneally, and two days later 100 μg of myosin in PBS was injected both intraperitoneally and intraveneously. Two days after the final immunization, the spleen cells were fused with Sp2/0-Ag 14 mouse myelomas (91). Hybridomas producing antibodies against myosin were screened by ELISA, and the final screening was performed by indirect immunofluorescence.

After cloning by limiting dilution, two hybridomas were established and named DM-2 or DM-6 (DM: Dictyostelium myosin). The monoclonal DM-2 antibody was mainly used in the present study. Whole sera of the positive mice were collected and used for the polyclonal control staining.

Immunoblotting: Sodium dodecylsulfate polyacrylamide gel electrophoresis (SDS PAGE) was performed according to Laemmli(55) on 10% slab gel, and the protein was electrophoretically transferred (102) to nitrocellulose paper (Bio Rad) for 22 h at 0.1 A (3 V/cm) in the buffer containing 25 mM Tris-base, 192 mM glycine, 0.1% SDS, and 20% methanol. The paper was blocked with 3% gelatin (BIO RAD), and sequentially incubated with DM-2 antibody [1:1 culture medium containing 3% BSA], TTBS [0.05% Tween-20 in Tris-buffered saline (pH 7.5)], peroxidase-labeled second antibody [HRPO-rabbit anti-mouse IgG (Litton); 1:330 diluted with TBS containing 3% BSA and 1% gelatin], TTBS, and finally with 0.5 mg/ml 4-chloronaphthol and 0.5 ug/ml H_2O_2 (30%) for color development.

Indirect Immunofluorescence: Cells at each development stage

were harvested and suspended in the phosphate buffer, and an aliquot of the suspension was placed on a cover slip. A thin agarose sheet [0.15 mm thick, 5x5 mm square wide, made of 2% agarose (immunological grade) dissolved in the phosphate buffer] was put on the cells. Excess buffer was removed using small pieces of filter paper, and the sample was observed under a phase-contrast microscope. When the cells were at the appropriate condition, the buffer was removed from the surface of the agarose until the cells became very flat due to the mechanical pressure. The samples were immersed in -15°C methanol and fixed for 5 min. After a brief rinse with PBS, the samples were incubated with the primary antibody [DM-2 culture medium or rabbit anti-chicken gizzard actin serum (1:20)] for 30 min at 37 °C. The samples were washed for 30 min with PBS (This washing was indispensable to prevent background staining). They were then incubated with FITC-labeled second antibody preadsorbed with Dictyostelium cell lysate.

The preadsorption was done as follows. The cell pellet (0.1 ml) was fixed for 5 min with cold methanol (-10°C), washed 3 times with PBS, and re-suspended in 500 ul of the second antibody [(1:25) diluted with PBS containing 0.1% (w/v) NaN_3; Cappel or Miles-Yeda]. The suspension was incubated for 30 min at 36°C, then centrifuged for 30 min at 13,000 rpm, and finally the adsorbed antibody was carefully collected using a Pasteur pipette. The adsorbed antibody could be kept for as long as one month in a refrigerator. The samples were finally washed with

PBS, briefly rinsed with distilled water, and mounted with Gelvatol (80) containing 1 mg/ml p-phenylenediamine (48). The fluorescent micrographs were taken under an Olympus epifluorescence microscope (BH-RFL) equipped with x100 lens (N. A. 1.25) using Kodak Tri-X film and developed with Acufine (Acufine, Inc.).

Preparation of Triton-insoluble ghosts: For SDS polyacrylamide gel electrophoresis, a suspension of cells was permeabilized with the P-buffer[10 mM PIPES, 50 mM KCl, 1 mM $MgCl_2$, 10 mM EGTA, 1mM DTT, 0.2 mM PMSF, (pH 7.6)] containing 0.5% Triton X-100 for 10min on ice. After 5 min centrifugation at 10,000 rpm, the pellet and supernatant were separated and boiled for a few min in SDS-sample buffer. Actin and myosin quantity was estimated using a Gelman densitometer.

For the contraction of the Triton-insoluble ghosts, aggregation-competent cells were overlaid with a thin agar sheet and treated with 10^{-6}M cAMP at 5°C. After 2 min, when the endoplasmic rods disappered as shown in result (3-b), the cells were permeabilized with P-buffer containing 0.5% Triton X-100 for 10 min at 0°C, then extracted with the P-buffer for more 5 min. P-buffer containing 1 mM ATP was applied to the Triton-insoluble ghosts resulting in contraction under a phase-contrast microscope.

IV. RESULTS

A. MICRTUBULES AND CELLULAR POLARITY

1. Microtubule System in Dictyostelium Amoebae

There are not so many works on microtubule system in Dictyostelium amoebae. Fig.1 shows a typical cell prepared by the agar-overlay immunofluorescence. All microtubules radiate from a single focus, termed as microtubule organizing center (MTOC) near the nucleus (54). A single amoeba of Dictyostelium discoideum (NC-4) contains about 30 microtubules and in the case of Dictyostelium mucoroides (Dm-7) 15 microtubules were observed. Each microtubules never terminated at the plasma membrane but rather turn to the endoplasm again. In a locomotory cell with a distinct pseudopode, some microtubules extend toward the pseudopode but rarely reach inside the hyaline region.

MTOC consists of a square core structure termed as nuclear associated body by Roos (81) and amorphous material surrounding the core. The observation by electron microscope proved microtubules initiated from the latter. Nuclear associated body, which corresponds to centriole in higher animal cells, duplicates and organize the spindle microtubules at mitosis.

Possible roles of cytoplasmic microtubules in a Dictyostelium amoeba are (a) retention of cell shape, (b) intracellular transport and (c) establishment of cellular polarity. The first role is suggested by the fact that disruption of cytoplasmic microtubules by microtubule inhibitors or cold temperature cause rounding up of cells. The second role is suggested by the observation that microtubules and unknown

vescicles linearly move to and away from the MTOC and sometimes show the saltatory movement. This movement was also inhibited by microtubule inhibitors also supporting the second role of microtubule system in Dictyostelium.

2. Relationship between Microtubules and Cellular Polarity

Some works on higher animal cells revealed that the centriole play an important role in determining the direction of cell locomotion (3, 40, 52, 64). To see if it is true or not for the amoeboid movement of Dictyostelium, the quantative study was performed using indirect immunofluorescence on aggregating cells (Fig.2). At this stage of the development, the cells migrate to the aggregation center forming streams, and we can inevitably identify their direction of locomotion. Furthermore, the agar-overlay method greatly improved the fixation of cells and made it possible to recognize MTOCs as well as nuclei by phase-contrast microscopy. By comparing the phase and immunofluorescent micrographs, the position of MTOCs and nuclei could be clearly determined in the total 693 cells. The frequency that the MTOCs were present in the anterior side of the nuclei was 52.5 % and the probability ($p < 0.01$) of Student's t test suggested that the specific localization was very significant.

However, there were not a few cases of MTOCs behind the nuclei. To ascertain the possible mechanism of MTOC in the direction of cell movement, the observation of the location of MTOC in living cells was done. Under the phase-contrast microscope, MTOC localizing near the nucleus could be identified

as a dark spot and around them various vesicles in cytoplasm come together as mentioned above. By taking photographs of individually locomoting cells every 30 sec for 5 min, the location of MTOC and nucleus was traced in 159 cells. Fig. 4 shows a typical trace of Dictyostelium amoeba. In about 60% of the observed cells, MTOCs were always located in front of the nucleus. But, at the same time, in about 15% of cells, MTOCs were located behind the nuclei for at least 5 min. In addition, in 7.5% of the observed cells MTOC's changed their location to the opposite side of the nuclei during the period of tracing. To follow the time course of the changes in location of MTOC and nucleus in locomoting cells quantitatively, the parameter given by dividing the distance from the anterior end of the cell to the location of the MTOC or the nucleus by the longitudial length of the cell was estimated in each observations (Fig. 5). This quantitative estimation clarified that the MTOC was always located at the center of the cell ($p = 0.5$), whereas the location of the nucleus continuously changed varied in a locomoting cell. The MTOC might play a role to fix the nucleus in the middle of the cytoplasm.

B. MICROFILAMENT SYSTEM IN DICTYOSTELIUM AMOEBAE

1. Cortical Localization

Actin and myosin, which are major force generating components of microfilament system are prevalent in Dictyostelium amoebae, representing about 8% and 0.5%, of the total cellular protein respectively (16). This content is comparable to that of other non-muscle cells, but no large scale of microfilament bundles were observed in Dictyostelium amoebae by electron microscopy. When Dictyostelium amoebae were treated with glycerol the cortical meshwork of microfilament were not extracted and prevalent as revealed by Fukui & Katsumaru (32). The cortical meshwork of microfilament was partially isolated by extraction of non-ionic detergent Triton X-100 by Greenberg et al (41). When cells attached to the coverslip were flushed away, microfilaments were observed to bind to the plasma membrane left as demonstrated by Clark et al(15). SDS PAGE of the plasma membrane fraction isolated according to Spudich(93) shows that actin and myosin are major components of plasma membrane fraction (Fig. 6), representing about 10% and 7-10% of the cell content respectively. Most of these proteins were released by treatment with ATP (Fig. 6). The study on the actin-binding activity of isolated plasma membrane indicated the participation of the membrane integral protein in the linkage of actin with the membrane (8,18,39,47,57,58). These observations refered to the idea that the microfilaments should have some connection with the plasma membrane assuming that the motile activity of non-muscle cells might be regulated by the mechanism analogous to the skeletal

muscle contraction system.

Fig. 2 shows the changes in the amount of protein in Triton -insoluble ghosts during the first 10 hours of the development. Triton-insoluble protein incresed abruptly during the first 2 hours, and then showed a decline for a while. It increased again during the aggregation stage and declined at the end of the aggregation. These changes in the Triton -insoluble protein are correlated with the changes in the rate of cell locomotion as described in Introduction. In the light of actin and myosin being the major components of the Triton-insoluble ghosts (see Result C-2), the amplification of the motile machinery might bring about more active movement of amoebae during early the development.

2. A Unique Microfilament Inhibitor: Dimethylsulfoxide

Cytochalasins, widely used microfilament inhibitors is known to be ineffective on Dictyostelium. Fukui & Katsumaru (32) found that dimethylsulfoxide (DMSO) acts on Dictyostelium cells to cause the dislocation of the cortical microfilaments from the plasma membrane resulting in cell rounding up, cessation of cytoplasmic streaming and impediment of cytokinesis . This section describes the detailed morphorogical changes induced with DMSO and the dissociation of actin and myosin from the plasm membrane. In addition, prominent filopode-like projections containing microfilaments were formed on a restricted portion of the cell surface upon the treatment with 5% DMSO for 2.5-5 min and corresponded to the anterior end of a migrating cell.

a. Morphological Changes induced with DMSO

Under phase-contrast or differential interference phase microscopy, the cells treated with 5% DMSO formed numerous projections immediately upon treatment (Fig. 8), and the cytoplasmic streaming, judging from the movement of the granules, abruptly ceased. By 5 min of treatment, the cells round up in shape and the projections free from the substratum shortened. At the same time, the number of the projections had markedly decreased. The cells resumed their cytoplasmic streaming in 20 min, and soon after this formed motile filopodes as well as pseudopode and started to migrate.

Because of the small size (7 μm in diameter), neither small projections nor the fine surface architecture of the cells could be identified under the light microscopy. This led us to perform the SEM studies to find that dramatic changes occurred on the surface of cells treated with 5% DMSO. The untreated cells migrated on the substratum at about 400 μm/h forming several to tens of long filopodes (Fig. 9a), which apparenly serve as cellular exploring organs as suggested by Albrecht-Buehler. By 2.5 min of treatment, numerous thin projections as well as a few large blebs were formed and the surface became very smooth in texture (Fig. 9b). Between 5 and 10 min of treatment, the extended projections shortened and decreased in number (Fig. 9c and d). After 30 min, virtually all of the projections had disappeared and the surface displayed a wrinkled texture again (Fig. 9e). In 60 min, the cells had reformed large pseudopodes and looked as though they were in locomotion (Fig. 9f). Under a

light microscope these cells could be clearly seen migrating. Interestingly, apparent exocytosis of vescicles as well as endocytosis of bacteria was prominent in cells which had regained their ability of locomotion, which was observed under a differential interference phase microscopy.

The DMSO-induced projections of cells treated for 5 min contained microfilament bundles similar to those observed in the native filopodes in thin sections (Fig. 10a-b). The unique feature of the projections was that they contained numerous ribosomes (Fig. 10c). It should be noted that the cortical microfilaments running parallel to the plasma membrane could not be observed in these cells. After 30 min, the cortical microfilaments returned to their location just beneath the plasma membrane and were apparently associated with the concave surfaces of the membrane (Fig. 10d).

b. Dissociation of Microfilaments from the Plasma Membrane

To examine the effects of DMSO on the membrane-bound microfilaments, the SDS PAGE analysis was performed on isolated plasma membrane fractions. The 42 and 210 Kdalton proteins obviously became dissociated from the membrane by treatment of the cells with 5% DMSO for 5-15 min (Fig. 11). The densitometry analysis showed that about 80% of the 42 K dalton protein was released from the membrane by the treatment with DMSO. These protein species most likely represented actin and myosin heavy chains respectively, since they co-migrated with isolated Dictyostelium actin and myosin heavy chains; and both were

dissociated from the membrane by ATP (See Result A-1), confirming the data of Spudich (93) and Condeelis (18). Futhermore, the 2-D gel electrophoresis (Fig. 12) showed that about 85% of 42 Kdalton protein had an isoelectric point identical to that of Dictyostelium actin (pI=5.6).

The amount of membrane-bound actin and myosin increased by the 30 min treatment with DMSO (Fig. 11d) or the removal of DMSO, supporting the data described above, namely, the cessation and resumption of the cytoplasmic streaming and the reversible changes in cell surface architecture. The application of DMSO to the membrane preparation was ineffective for dissociating actin and myosin from the plasma membrane (data not shown).

c. Restricted Localization of the DMSO-induced Projections and Its Correlation with Cellular Polarity

The most dramatic feature observed in cells treated with 5% DMSO for 2.5-5 min was that the filopodelike projections formed in a restricted portion of the cell surface (Fig. 13). The SEM observation that a great number of the cells displayed surface differentiation led us to speculate on the possible correlation of the cellular polarity. The finding that colloidal gold particles attached to the cell surface accumulated on the tail end of migrating cells encouraged us to assess this idea by the phagokinetic track technique of Albrecht-Buehler (2). In Dictyostelium, the application of E. coli, instead of gold particles, on cover slips provided the best results.

The cells engulfed the bacteria, digested them, and performed cell divisions forming branched phagokinetic tracks

(Fig. 14). In many cases, formation of the DMSO-induced projection region was observed on the head portion of a migrating cell (Fig. 15). The apparently immotile cells which had no tracks sometimes formed the projections on their lower part facing the substratum as shown in Fig. 9c. The frequency of the formation of the projection region was quantitatively estimated in relation to the direction of cell locomotion and diagrammatically represented in the inset of Fig. 15. The Student's t test of the probability ($P<<0.01$) strongly suggested that the formation of the DMSO-induced projection region at the head portion of the cells was significant.

3. Localization of Actin and Myosin Using Improved Immunofluorescence

This section documents the localization of actin and myosin in various developmental stages of *Dictyostelium* by the improved immunofluorescence using rabbit anti-actin and newly obtained monoclonal anti-*Dictyostelium* myosin antibodies. Actin and myosin were showed to be localized at the cortical region and change the distribution correlated to the cell activity. Actin and myosin stainings were observed at the posterior cortex of the migrating amoebae, whereas only actin stining was localized at the anterior pseudopode. This finding suggested that the motive force of amoevoid movement is generated at the posterior cortex of a migrating cell.

a. Specificity of Antibodies

The antibody of DM-2 hybridoma was of the IgG class as shown by the Ouchterlony double diffusion test (data not shown), and the specificity was tested by immunoblotting. DM-2 antibody was reactive to the heavy chain of purified Dictyostelium myosin (Fig. 16-c,g) as well as the corresponding band in the whole cell lysate (Fig. 16-b,f). However, DM-2 did neither crossreact with rabbit skeletal muscle myosin (Fig.16-d,h) nor chicken gizzard smooth muscle myosin (210K band in Fig.16-a,e).

In the initial experiments, some minor bands ranging 170-180 K represented positive reaction with DM-2. Adding protease inhibitors to the purification buffers [(50 ug/ml leupeptin, 1 mM PMSF (phenylmethylsulfonylfluoride), and 0.1 mM TLCK (p-tosyl-L-lysine chloromethyl ketone hydrochloride)] could not totally eliminate the contamination of these minor bands from the myosin preparation. These bands were likely to be degradation product of myosin heavy chain since the amount of these proteins included in the whole cell lysate decreased significantly by solubilizing the cells by adding pre-warmed SDS-sample buffer to the cell pellet (Fig. 16-b).

The specificity of the immunofluorescence was tested by several control experiments including (a) the staining without the primary antibody or (b) with pre-immune mouse serum for the primary antibody. In the initial experiments, some background staining was occasionally observed even by the control staining. This non-specific staining was apparently caused from the second antibody, and could be eliminated by the pre-adsorption of the fluorochrome-labeled antibody with Dictyostelium lysate as

described in Materials and Methods.

b. Preservation of Cell Structure by the Agar-overlay Technique

Migrating Dictyostelium amoebae are not large enough (8 μm in diameter) or flat enough to allow light microscopic observation of their cellular structures, as shown by scanning electron microscopy (see Fig. 9a). Futhermore, their cytoskeletal machinery are very small and no stable large structures (such as stress fibers) are visible. In addition, their cytoskeletons are susceptible to the mechanical disturbances which are inevitable during preparation of samples for immunofluorescence. These problems were overcome by laying a thin agarose sheet over the cells before fixation and performing the immunofluorescence procedure under this condition. The amoebae could migrate normally and undergo aggregation under the agarose sheet. Microscopic images of the cells improved greatly with this technique, and cellular organelles such as pseudopodes, mitochondria, nuclei, nucleoli, and nuclear-associated bodies could be identified under a phase-contrast microscope. In addition, the mechanical support by the agarose sheet resulted in good preservation of the micro- as well as macro-morphorogy of the cells, as shown by comparative phase-contrast microscopy before and after fixation with cold methanol (Fig. 17)

c. Actin and Myosin in Vegetative Cells

In the vegetative stage, the cells feed on E. coli, divide

by binary fission every 3 hrs, and show a round shape with a few small pseudopodes. Actin staining caused a diffuse fluorescence all over the cytoplasm, whereas anti-myosin specifically stained the peripheral of the cells (Fig. 18 a-d). The different distributions of actin and myosin were not unexpected, since cortical motile activity is not prominent at this stage and the cortical machinery is likely to be organized in parallel with the activation of motile event. This idea was supported by the observed changes in the pattern of the actin staining during the transformation from vegetative to migratory amoebae; both actin and myosin stainings were evident at the cortex at this stage (Fig. 18 e-h).

To assess the possible involvement of actin and myosin in specific motile activities, special attention was paid to the cells performing cytokinesis or phagocytosis. The polar pseudopodes in dividing cells were stained with anti-actin (Fig. 18 i,j). However, very specific staining with anti-myosin was observed at the constricted region of the dividing cells. Interestingly, this myosin staining showed a filamentous structure alighed parallel to the axis of constriction (Fig. 18 k,l), although no specific actin-containing structure was seen in this region (Fig. 18j). Staining of the phagocytotic apparatus was similar to that of the anterior pseudopode; i. e., brightly stained with anti-actin, but not with anti-myosin (Fig. 19).

d. Actin and Myosin in Locomotory Cells

When the amoebae were harvested and inoculated onto the agar plate, they started active locomotion in 2-3 hrs. At this stage,

both the anterior pseudopode and the posterior cortex were stained with anti-actin whereas only the posterior cortex was stained with anti-myosin (Fig. 20 a-d). Clearly, two classes of anterior pseudopodes were present, appearing as dark and light regions under a microscope equiped with dark-contrast phase optics. The dark region was stained strongly with anti-actin but the light region was not. The light pseudopode looked like a hyaline region, and the boundary between this region and the ground cytoplasm (granuloplasm) showed actin staining which might be due to a cortical actin layer (arrow head in Fig. 20f). The differences in the staining of pseudopodes may indicate differences in the actin organization of these pseudopodes.

In cells in contract with each other, the conact sites were stained strongly with anti-actin (Fig. 20 g,h), Whereas no staining was observed with anti-myosin. This may be due to the well-developed microfilament mesh found by transmission electron microscopy (see Fig. 3c of ref.32). The periphery on the other side of the contact region was specifically stained with anti-myosin (Fig. 20 i,j).

e. Actin and Myosin in Aggregating Cells

In the aggregation stage, when the amoebae aggregate in streams, elongated cells migrate forming head-to-tail as well as side-by-side associations. In this stage, not only the pointed pseudopode and posterior region but also the lateral cortical region was stained with anti-actin (Fig. 21 a, b). Anti-myosin only stained the lateral and the posterior cortex (Fig. 21 f,g).

In the tip of the pseudopode, peculiar rod-like staining with anti-actin, not seen in other stages, was prominent (Fig. 21 c,d).

We obtained good macroscopic images of the aggregate by the agar-overlay technique (Fig. 21 a-e). Very bright myosin staining was particularly observed at the posterior end next to the lateral cortex of the cells at the periphery of the aggregate (Fig. 21e). This myosin staining suggested that a centripetal force was generated at the outermost cortex of the peripheral cells and this force might be required for the formation of the aggregate. This idea was supported by evidence for myosin localization in contacting cells which looked as though they were pushing each other (Fig. 20j).

C. IDENTIFICATION OF MYOSIN THICK FILAMENTS IN SITU AND A REVERSIBLE CHANGE IN DISTRIBUTION IN RESPONSE TO CHEMOTACTIC STIMULATIONS

1. Identification and Localization of Myosin Thick Filaments in vivo.

"Agar-overlay" immunofluorescence technique which enabled us to localize tubulin, actin, and myosin in Dictyuostelium, was modified in the present study. A monoclonal antibody against Dictyostelium myosin (DM-2) recognized the heavy chain of purified myosin descrived above. Immunogold staining of purified Dictyostelium myosin showed that DM-2 was reactive to reconstituted myosin thick filaments (Fig. 23b). The newly improved fixation protocol (fixation using methanol containing 1% formalin) rewarded us with a very specific view of rod-like shapes (Fig. 23c). The rods were uniform in size (0.1-0.2 μm wide, 0.7 μm long) and identical to those found with immunofluorescent staining of reconstituted thick filaments of purified Dictyostelium myosin (Fig. 23d). It was ascertained that the presumptive myosin rods were localized at the cortical region of vegetative cells as shown by the fluorescence micrographs taken at several focal planes (Fig. 24 a-d).

The fixation seemed to be appropriate, and the myosin rods likely reflected the in situ form of the molecules since: (a) the samples were fixed instantaneously in cold methanol containing formalin, and (b) once fixed, the rods did not dissolve even when PBS was replaced with the myosin-solubilizing solution containing 0.6 M KCl. However, no thick filaments could be found in transmission

electron microscopy of thin sections of the cells prepared for the immunofluorescence. Encouraged by the finding of the rod-like fluorescence in the cells, I investigated the possible disruption of the thick filaments by the fixation (Table 1) and found that this did occur. The fixation with 0.1% OsO_4 for 10 min at 4 C destroyed the rod-like structures leaving only weak dot-like fluorescence. Thus the non-muscle myosin thick filaments are probably susceptible to chemical fixation, which might be the reason for much argument about the presence or absence of non-muscle thick filaments.

A vegetative cell performs cytokinesis every 3 h. At this stage, the cortical fluorescence mostly disappears except in the portion of the cleavage furrow. The myosin rods are aligned in parallel with each other forming a circular and peripheral ring-shaped fluorescence (Fig. 24 e-h). This information suggested the presence of a contractile ring(88) of microfilaments at the constricting portion of the dividing cells, which have never been observed by electron microscopy.

When the amoebae are compelled to start development, their motile activity increases. During the initial 2 h of development, myosin rods increased in number and appeared in the endoplasm side by side within the cortex (Fig. 24k, 25a). In polarized cells performing directed locomotion with the anterior pseudopode, the rods had accumulated in the posterior cortex. Occasionally, some linear alignments of the rods were evident just beneath the cortex (Fig. 24 i-k). This evidence supports the idea that the force for the amoeboid movement is generated by contraction of the posterior cortex.

2. Translocation of Myosin Rods in a Chemotactic Response.

The assembly of *Dictyostelium* myosin is beleaved to be regulated by phosphorylation of its heavy chain, and dephosphorylation would cause the monomeric myosin to form thick filaments with a large amount of actin-activated ATPase, in contrast to the case of mammalian myosins(90). Malchow et al(61) found that the addition of a chemoattractant cAMP to the aggregation-competent cells induced the rapid and transient phosphorylation-dephosphorylation cycle of myosin heavy chains. Do thick filaments perform cyclic changes of disassembly-assembly in response to the cAMP signal? I found that the myosin rods disappeared from the endoplasm and accumulated at the cortex in 2 min after treatment with 10^{-6} M cAMP at 5°C. Futhermore, this specific localization of the rods resumed spontaneously in one more minute (Fig. 25 a-c). The change in the distribution of myosin rods were very dramatic and was observed in almost all of the cells within 1 min after the addition of cAMP at 11°C; This response was too rapid to be followed at 23°C.

McRobbie & Newell(69,70,71) recently reported a transient increase of the Triton X-100 insoluble cytoskeleton in response to cAMP. Then immunofluorescence using anti-actin antibody was performed on responding cells. The actin staining was localized at some cortical region such as pseudopode, posterior cortex and hyaline in normal aggregation-competent cells described above. When cells were treated with cAMP, cortical actin staining increased uniformly (Fig. 26).

Vegetative amoebae show chemotaxis toward folic acid(76) which is released from E. coli. Malchow et al(61) claimed that the transient phosphorylation of myosin heavy chain could be monitored when folic acid was added to the suspension of vegetative cells. To consider this probability, I prepared the cells in response to 10^{-4} folic acid for immunofluorescence using anti-Dictyostelium myosin (DM-2). Myosin rods, which was localized at the cortex in a vegetative cell(Fig. 24), appeared in the endoplasm after 3 min of addition of folic acid and resumed in one more min (Fig. 27). Interestingly , cAMP induced identical changes with folic acid, too (Fig. 27).

How can the cell transmit the chemoattractant signal into the cytoplasm? Some transient responses have been revealed occurring in response to the chemotactic stimulation, such as influx and eflux of calcium ion, decrease of extracellular pH and increase in the levels of intracellular cGMP as well as cAMP. Malchow et al.(62) showed that a microcapillary containing calcium ionophore A23187 caused a cell contraction and extention of pseudopode toward the tip of microcapillary. However, I would exclude the possibility of the influx of extracellular calcium ion as a triger of the chemotactic response by the observation of normal chemotactic response of myosin rods even with 5 mM EGTA in extracellular phosphate buffer. However, the calcium ionophore in the solution containing Ca^{2+} induced the transient translocation of the myosin rods. Cytoplasmic rods disappeared and cortical rods were accumulated after 3 min of the addition of the ionophore to the aggregation competent cells and this localization of the rods resumed in one more minute (Fig. 28 c-d). Futhermore,

when vegetative cells were treated in the same way, myosin rods appeared in endoplasm after 3 min of the addition of ionophore and the cortical distribution resumed, in one more minute at 5 °C (Fig. 28 a-b). These response of the amoebae to the ionophore could not be observed in the absence of extracellular calcium. The evidence indicated that cAMP and folic acid, which didn't share common receptors on cell membrane(105), increased the intracellular calcium ion concentration. Therefore, it is possible that the local attachment of the chemoattractants to their receptors on cell surface might induce a local influx of calcium ion, which lead to a local activation of movement resulting in chemotactic movement.

A cell responding to cAMP contracts rapidly. If cAMP is applied locally, the cell extends a pseudopode in the direction of the signal within several seconds(37). The present study suggested that the translocation of the endoplasmic myosin rods was coincident with this response to a chemotactic stimulus. Since the accumulation of rods in the cell cortex was a transient event, the question whether a cell without the endoplasmic rods could contract arose. We prepared Triton-insoluble ghosts of the cells with the endoplasmic rods depleted by treatment with cAMP, and examined their contractility in response to cAMP. SDS-gel electrophoresis showed that the ghosts were mainly composed of actin and myosin comprising up to 25% and 50% of the total cellular proteins (Fig. 29f). When 1 mM ATP was added to the ghosts, the cortex contracted in a few seconds (Fig. 29 d,e). The result suggests that the cortical myosin rods might be

organized in a manner appropriate for generating the force required for the amoeboid movement.

V. Discussion

1. Assessment of the Agar-overlay Technique

Extraction of plasmodium placed between two sheets of agar with glycerol was first reported with Physarum polycephalum (50). This method was recently applied for the immunofluorescence of Physarum plasmodium and was shown to be efficient for providing good immunofluorescent images (73). The present study showed that the agar-overlay technique is very useful for either phase-contrast or immunofluorescent microscopy of Dictyostelium amoebae as small as 8 um in diameter. The possible drawback of this technique is an artifact arising from mechanical stress from the agarose, which might cause peripheral staining of actin and myosin. To circumvent this problem, the staining patterns of flat cells prepared by the agar-overlay technique was compared with those of round cells prepared by conventional fixation procedure. Fixation with cold methanol totally disrupted the structure of suspended round cells. Thus, conventional fixation with 3.7% formaldehyde in PBS or 15 mM phosphate buffer is not suitable because it results in drastic shrinkage of the cells. Careful reconsideration of the fixation protocol for suspended cells showed that fixation with 2.5% formaldehyde in the phosphate buffer for 10 min followed by extraction with -15°C methanol for 5 min resulted in good preservation of the cellular morphology. Actin and myosin were also localized mainly at the cortical region of the suspended cell (Fig.22 a, b). This observation, together with the evidence that the amoebae could undergo normal aggregation, encouraged me to apply the agar-overlay technique for the immunofluorescence. I were rewarded with well-preserved

cellular structures and high resolution in fluorescent images.

2. Evaluation of the Fluorescent Staining

Cellular structures were well preserved by the agar-overlay technique despite of the fact that no strong cross-linking fixatives are allowed in immunofluorescence. The good preservation probably resulted from (a) rapid fixation by dipping the samples into cold methanol and (b) the preservation of disruption during the staining steps.

I next considered whether the crescent-shaped fluorescence by monoclonal DM-2 antibody reflects the specific supramolecular architecture of myosin, since monoclonal antibodies only recognizing specific epitopes are not unusual (25). I found that the staining patterns by polyclonal anti-myosin sera were essentially identical to those by DM-2 (Fig.22 c,d). This indicated that the fluorescence by DM-2 must correctly reflect the localization of myosin.

Several different patterns were observed in the staining with polyclonal anti-actin. Very dense patch-like fluorescence (Fig.20) might reflect the well-developed microfilament meshworks revealed by electron microscopy (see Fig.3-c of ref.32). Peripheral staining might represent the loose microfilament layers localized beneath the plasma membrane (see Fig.3-D of ref.32). The diffuse fluorescence in the cytoplasm by anti-actin probably reflect the loose cytoplasmic mesh of microfilaments (represented by Cf in Fig.2 of ref.). The diffuse fluorescence probably does not reflect the monomeric form of actin, since soluble proteins

are not likely to remain after the methanol fixation. Thus, the differential patterns of fluorescence seem to represent the different modes of organization of actin filaments. This notion was also supported by the following data. Recent study using fluorescence-conjugated phalloidin, which speciffically bind to only filamentous actin, showed same staining patterns as actin antibody.

I recognize that I must carefully evaluate the influence of the accesible volume (4) on the amount of fluorescence. For example, I cannot exclude the possibile function of the difference in the pathlength caused by the included organelles (excluded volumes), although the thickness of the cells is mostly constant because of the overlaid agarose. However, the totally different staining patterns of actin and myosin and the difference in the anti-actin staining in some pseudopodes (Fig. 20-e,f) suggest that the amount of the fluorescence could not be totally, if any, interpreted by the accessible volume.

This paper described the myosin rods in Dictyostelium amoebae by improved fixation. Following reasons implied that they are myosin thick filaments in situ.

(1) These rods were only structures in situ specially bound with monoclonal anti-Dictyostelium myosin.

(2) The dimension of these rods was same as that of reconstituted myosin thick filaments in vitro.

(3) These rods were localized at specific region and somtimes showed linear alignment.

(4) These rods were translocated and reorganized in response to chemotactic stimulation.

(5) An average cell should contain approximately 3.8 $x10^{-10}$ mg myosin assuming that each cell has 7.5 x 10^{-8} mg protein and myosin represents 0.5% of the total cell protein (93). This myosin is equivalent to 5 x 10^5 myosin molecules. Assuming that about 75% of the molecules formed thick filaments, as suggested by the in vitro phosphorylation experiment (53), and each thick filament was composed of 30 molecules, a cell would have about 1.3 $x10^4$ thick filaments. This number meets well the pictorial view shown in Fig.24.

Many workers have ever wrestled with the problem of the existence of myosin thick filaments in non-muscle cells. Although immunofluorescent studies have ever described the overall distribution of myosin within non-muscle cells, myosin thick filaments have never been observed using not only immunofluorescence but also routine electron microscopic methods. Following reasons why myosin thick filaments were invisible in non-muscle cells have ever been elevated.

(1) Since myosin assemble to form thick filaments transiently during generating force as mentioned in smooth muscle, it is difficult to identify myosin thick filaments in vivo (90).

(2) The number is very few and if they were randomly orientated, most would be cut obliquely, making identification difficult(74).

(3) Myosin exists as smaller aggregates or oligomers than thick filaments reconstituted in vitro(49,109).

(4) Myosin thick filaments are not well preserved during the conventional fixation.

In this paper myosin rods were observed in Dictyostelium amoebae in all situations i.e., motile or resting, vegetative or developing and so on. Moreover, these rods turned out to be sensitive to OsO_4 conventionally used for electron microscopic preparations. The susceptibility to chemical fixations might explain the difficulty of the study of myosin thick filaments in non-muscle cells. Since thick filaments are observed in Amoeba fixed with OsO_4 (72,78,94), these filaments might have different sensitivity to chemical fixations.

3. Correlation Between Cellular Polarity and Cytoskeleton

Locomoting Dictyostelium amoebae have a morphological polarity, with a granule-free pseudopode at the front and a tail at the posterior. This polarity represents the current direction of locomotion by the cell. This makes it possible to judge the direction of locomotion of a fixed cell for immunofluorescence. Experiments using microtubule inhibitors and DMSO elucidated that both microtubule and microfilament systems play important roles on the determination of cell shape. These cytoskeleton also must take part in determining the morphological as well as the behavioral polarity. Apparently, biased microfilament system was observed in a locomoting cell. Both actin and myosin stainings were observed at the posterior end, whereas only actin staining, at the frontal end. The possible roles of actin and myosin at different regions will be discussed in the following chapter.

Albrecht-Buehler(3) built up a hypothesis that the MTOC in front of the nucleus plays an important role of the determination of cell locomotion controlling the spatial distribution of

microtubules in the cytoplasm. This hypothesis is supported by some evidences in higher animal cells (3,40,52,64). This paper described that MTOC in front of nucleus was highly frequent in Dictyostelium amoebae. However, the MTOCs apparently behind the nucleus or showing a change in position were observed in this study. This may indicate that the importance of positioning of MTOC in front of nucleus is not essential for Dictyostelium amoebae. The result of Fig.5 alternatively show that the possible role of MTOC is sustaining a nucleus in the middle position of a cell. However, the hypothesis that MTOC in Dictyostelium may take part in the determination of cell locomotion will not be denied in the present study.

This study showed that the DMSO-induced projections were formed in a restricted region of the cell surface. The uneven distribution of the projections probably did not result from their lateral movement, because Filosa & Fukui(29) demonstrated that the capping of surface receptors was reversively inhibited by DMSO. The uneveness seems to reflect in situ uneveness of the cellular organization. This result was not unexpected from the observation of a local increase in the amount of actin at the anterior pseudopode. This presumption was supported by the result of the "phagokinetic track" experiment.

4. Significance of Differential Organization of Motile Machinery

a. Significance of interaction between actin filaments and cell membrane

The treatment of DMSO on Dictyostelium amoebae induced the

cessation of cellular locomotion and cytoplasmic streaming, rounding up of cells and inhibition of movement of lentil receptors on cell membrane. These phenomena were perhaps resulted from the dissociation of cortical microfilaments from the cell membrane. The major components of the dissociated microfilaments were found to be actin and myosin. Moreover, after 20 min of the treatment or after removal of DMSO, cells resumed their cytoplasmic streaming and started to migrate. By this time, cortical microfilaments resumed to bind the cell membrane. These observations indicate important roles of microfilaments bound to cell membrane in the maintenance of cell shape, cell locomotion, cytoplasmic streaming and movement of cell surface receptors. Molecular basis of biological action of DMSO, which is not clear at the present time, is thought to be the result of dissociation of actin filaments from the actin binding protein in cell membrane by working directly on the membrane or changing intracellular ionic condition.

In cells treated with DMSO, the two different classes of cortical microfilaments could be obviously seen in thin section: those of the first class had become dissociated from the cell membrane, whereas those of the other class remained at the membrane and were eventually involved in the induced projections. Two types of contact sites between microfilaments and cell membrane are identified in the brush border of intestinal epithelial cells(45) and, recently, Dictyostelium cells(8,39): (1) an end-on attachment between the barbed end of actin filaments and cell membrane; and (2) lateral attachment mediated by rod-shaped bridges. End-on contacts between

microfilaments and cell membrane occurred with highest frequency in cortical meshworks. These end-on contacts of dense cortical meshworks, which were often seen in an anterior pseudopode, might take part in building normal filopodes or filopode-like projections induced with DMSO at the anterior region of amoeba.

b. Correlation between cell motile activity and motile machinery during early development

Motile activity of Dictyostelium amoebae shows drastic changes during early development. Vegetative cells have lower motile activity, feeding on E. coli and dividing every 3 hrs. Removal of E. coli makes cells initiate their development and invoke active locomotion. The rapid increase in the Triton-insolubule cytoskeleton by 2 hrs after the initiation of development indicates that the enlargement of cellular motile machinery may result in the increase in cell motile activity.

Fig 30. shows shemata of Dictyostelium amoebae at various stages stained with anti-actin and anti-myosin antibodies. Actin of vegetative amoebae showed diffuse staining in the cytoplasm, whereas myosin was localized at the cortex but their number was much smaller than developmental cells. During the initial 2 hrs of development, actin staining became strong and localized at the cortical region; on the other hand, myosin rods increased in number and appeared in the endoplasm side by side within the cortex. These observations indicates that the increase of cortical microfilament system brings about the enlargement of cell motile machinery as described above. The appearance of

myosin rods in the endoplasm may be explaned as 'active state' of amoeba in the light of the facts of going and coming of myosin rods between the endoplasm and the cortex in developmental cells.

c. The Localization of Motile Machinery at the Tail Cortex in Dictyostelium Amoebae

By 5-6 hrs of the development, Dictyosteliium amoebae aquire morphorogical polarity; monopodial cells with anterior pseudopode and posterior tail. Functional differentiation of motile machinery is apparent in these cells: (1) Actin staining was seen in the pseudopode but myosin staining was not; and (2) both actin and myosin staining were accumulated at the tail cortex. Such colocalization of actin and myosin at the posterior cortex indicates the interaction (e.g., contraction) of actin and myosin at this region, supporting the idea originally proposed by Mast for Amoeba (67). Actin filaments may form loose meshworks or bundles at this region and participate in the generation of force similar to 'sliding filament theory' mechanism (46) in muscle. These contractile gel composed of actin and myosin at tail region may contract by solation-contraction coupling (42) and solated endoplasm will be pushed forward to produce streaming.

Only actin staining was observed in a pseudopode. Some pseudopodes were not stained with anti-actin antibody but, alternatively, the boundary layer between hyaloplasm and granuloplasm was stained. These differences of actin staining of pseudopodes might be explained as the sequential changes of organization of microfilaments on the process of extention of

a pseudopode. A part of these actin staining at least must take part in the binding between cell body and the substrate to produce the motional friction. Such dense actin staining are also observed in the ruffle region in motile vertebrate tissue culture cells. This indicates a possible common function of actin filaments at the frontal region of motile cells. Fig. 31 shows the current model of amoeboid movement in Dictyostelium. This model shows the possible coupling of the tail contraction, the extention of pseudopode and changes of attachment sites on the substratum. The differential organization of cytoskeletal elements in the cell cortex must be related to the multi-forms of the regulatory components. Cortical distribution of some actin binding proteins have been reported by Condeelis et al(21) and Brier et al(13). Bazari & Clarke (7) have reported on calmodulin localization in the cortical region. Agar-overlay technique should be useful for the studying the differential distribution of these regulatory components in the cell cortex.

5. Correlation Beteen Contraction of Amoebe in Response to Chemotactic stimulation and Translocation of Myosin Rods

In early aggregation phase, Dictyostelium amoebae are attraced to the center responding to pulsatile signal of cAMP. The movement of the cells is periodic and highly organized. They move inwardly in steps, advancing for about 2 min and then stopping and rounding up for 5-7 min before moving again. Rounding cells are in refractory period, guaranteeing the one-dimensional guidance in the pulsatile waves of cAMP(101).

Dark-field microscopy visualized the coordinated movements as light and dark bands that form spiral or concentric circular patterns about a center. Dark bands were composed of moving cells and light bands were composed of respoding cells. These changes of cell shape in response to cAMP were also observed as changes of optical density in suspension of cells(36). Some workers tried to investigate the chemotactic responsibility of a single cell(33). When cAMP in a microcapillary was applied to a single cell locally, peudopode was extended to the microcapillary in no more than 5 sec at room temperature(37). Application of cAMP to a whole cell induced to the contraction of cell instead of the extention of a pseudopode.

a. Translocation of myosin rods may be mediated by their depolymerization and polymerization

This paper described the rapid transient translocation of myosin rods in response to chemoattractant of Dictyostelium. Myosin rods were seen within endoplasm as well as at cortex in aggregation-competent cells. The application of cAMP to these cells induced transient disappearance of endoplsmic rods and their accumulation to the cortex. Myosin rods described in this paper had the same dimension (0.7 μm length) of reconstituted purified myosin thick filaments in vitro. Some excellent mechanism for such large rods to translocate freely within a cell of 8 μm in diameter may be exist. Futhermore, two observations: rapid transient phosphorylation and dephosphorylation of myosin heavy chain during chemotactic response(61) and the tendency of polymerization of dephosphorylated(53) myosin indicate the

possibility that the tanslocation of myosin rods may be mediated by their depolymerization and polymerization, which perhaps may be controlled by phosphorylation and dephosphorylation of heavy chain. When cAMP binds to the receptors on the cell membrane, myosin thick filaments within the endoplasm may depolymerize and next polymerize at the cortical region.

Reappearance of myosin rods within endoplasm after 3 min of the addition of cAMP might be the result of the ATP-dependent sliding of actin and myosin. This idea is supported by the following observations: (1) Myosin bound to isolated cell membrane is released from the membrane with ATP and; (2) Uncoupler, DNP (35)or NaN_3 (24)which rapidly decrease ATP content of cell to about 5% and inhibited the chemotactic response inhibited the reappearance of myosin rods within the endoplasm (data not shown).

The rapid transient translocation of myosin rods was also observed in responding vegetative cells to folic acid and cAMP. Cortical rods were translocated to the endoplasm and then returned to the cortex. Phosphorylation and dephosphorylation of myosin heavy chain were also reported during this response by Malchow et al(61). Inhibition of the translocation of myosin rods to the endoplasm by DNP or NaN_3 (data not shown) indicate that the process might be ATP dependent contraction of actin filaments and myosin. However, caution must be paid to this interpretation because intracellular ATP is also substrate of myosin heavy chain kinase and precursor of cAMP. Inverse translocation was seen in vegetative cells and aggregation cells. This might be explained

by the differential localization of myosin heavy chain kinase or phosphatase.

b. Ca^{2+} triggers the translocation of myosin rods

The translocation of myosin rods was also induced with calcium ionophore. This induction was dependent on extracellular calcium, which does not support the possibility that calcium ionophore directly activates adenyl cyclase to increase extracellular cAMP. Alternatively, increase of intracellular calcium ion must be induce the chemotactic response. Even when extracellular calcium ion was depleted by EGTA, cAMP induced the rapid translocation of myosin rods in an aggregating cell. This observation prefers the influx of Ca^{2+} from an unkown intracellular reservior to the influx of extracellular Ca^{2+} as soon as cAMP binds to the receptors on cell membrane. The changes in the distribution of myosin rods were not also influenced by the extracellular Ca^{2+} in a vegetative cell responding to folic acid. Folic acid and cAMP are known to bind to different receptors(105). Neverthless, their binding to the receptors induced the increase of intracellar Ca^{2+}. Two possibilities may explain the identified 'transient' response by the ionophore similar to chemoattractant: (a) Ca^{2+} works as a trigger and the subsequent events proceed spontaneously; (b) response continues during the increase of intracellular Ca^{2+} until Ca^{2+} is eliminated from the cytoplasm. In the case of ionophore, probably the ionophore must be eliminated rapidly because cells started to locomote normally soonly after the contraction. Recently, Maruta et al. (66) reported that

Ca^{2+}/calmodulin inactivated some of myosin heavy chain kinase. It must be elucidated the role of calmodulin in the translocation of myosin rods described in this thesis.

6. Speculative Mechanism of Chemotactic Movement

This paper describes the overall distribution of motile machinery in Dictyostelium amoebae and the translocation of myosin rods in response to chemotactic stimulation. These informations would make it possible to reconsider the mechanism of amoeboid movement. The processes that a round cell having non-polar morphology responds and extends a pseudopode toward a local chemoattractant source and aquire the polar morphology (having a pseudopode at the front and a tail at the rear) may offer a simple system to understand amoeboid movement.

A round cell does not have extremely biased distribution of actin and myosin. When cAMP in a microcapillary is applied to the local region of the cell, cAMP will bind to receptors on local part of cell membrane near the microcapillary. The binding of cAMP on receptors will prompt the efflux from Ca^{2+} reservior directly or through unkown transmitter resulting in the local increase of Ca^{2+} concentration (perhaps at the cytoplasm near the side of microcapillary). The local Ca^{2+} increase will induce the depolymerization of myosin thick filaments at this region and polymerization of myosin at the distal cortex (perhaps at the cortex on the opposite side of the microcapillary)resulting in the accumulation of myosin thick filaments at this region. Futhermore, ATP-dependent sliding

between actin filaments and myosin will induce the contraction of the cortex at this region, by which endoplasm will be pushed forward toward the microcapillary, resulting in the extention of a pseudopode (Fig.31). Of course, It is prerequest that the local increased Ca^{2+} in the cytoplasm near the side of microcapillary will induce the solation of actin microfilaments at the front region. By this point this cell will aquire a distinct morphological polarity, with a granule-free pseudopode at the front and a tail at the rear.

To elucidate the possible mechanism described above, cAMP was applied to an extremely elongated cell which already aquire the morphological polarity. The front of such a cell is known to be more sensitive to stimulation by chemoattractant than the tail(96). This asymmetry in responsiveness is explained as the selectively localized receptors or the developed system of transmission at the front. Myosin rods disappeared at the frontal endoplasm of such an elongated cell responding to cAMP (data not shown). This observation supports the idea described above. Probably the cyclic translocation of myosin rods (the translocation and accumulation of myosin rods to the tail cortex, contraction of a tail and resulted in relocation of myosin rods) must be occurred partially in a normal non-chemotactic locomoting cell. However, cAMP-receptor complexes will not take part in such locomotion of a cell. Spontaneous increase of Ca^{2+} at the frontal cytoplasm, which was observed in Amoeba cell(99), may play a same role as in a chemotactically stimulated locomotion of a cell.

7. Future Challenges

Indirect immunofluorescence is one of the most useful methods for the study on the distribution of molecular components in the cell. However, since Dictyostelium amoebae are very small and not flat in shape, the conventional procedures for the indirect immunofluorescence have not been successful. They seriously destroyed the cellular structures. Agar-overlay technique described in this paper did overcome these deficiencies and provided us the excellent image of the Dictyostelium cytoskeleton. The distributions of tubulin, actin and myosin were determined by this technique in this paper. However, to elucidate the mechanism of amoeboid movement in more detail, it is necessary to clarify the function and dynamics of minor but important regulatory factors. Using the "agar-overlay" technique to investigate the intracellular localization of these regulatory factors, we will be able to gain the profound insight into the organization of the cell motile machinery.

Microfilament system were localized at the cortical region in Dictyostelium amoebae. Microfilaments are thought to bind to some integral membrane proteins. The identification of these proteins and the control of binding and releasing between microfilaments and membrane will be one of the central problems in the study of cell motility. Recently , receptors of chemoattractant bound to the cytoskeleton after the extraction of Triton-X 100 have been reported(34). The characterization of transmembrane proteins which form a connection between receptors and cytoskeleton will be important to elucidate the mechanism

of changes of cytoskeleton in response to chemotactic stimulation.

In this thesis, I described the rapid transient changes in the distribution of myosin rods in response to chemotactic stimulation. Application of immunoelectron microscopy is an urgent demand to elucidate that myosin rods are myosin thick filaments only when this technique may verify it.

One of the important objects is the molecular mechanism of the process between the binding of chemoattractant to receptors and increase of intracellular Ca^{2+}. Do the second messanger ever exist except Ca^{2+}? Intracellular cGMP(36), cAMP(38,82) and pH (63) are known to change in response to chemoattractant in Dictyostelium. It is interesting to know how these factors take part in the chemotaxis.

To reveal a presumptive Ca^{2+} sequestering system must be important for not only the total understanding of cell motility but also of cell differentiation. The crucial role of calcium in cell differentiation is supported by the observation of drastic changes in intracellular Ca^{2+} during the early development and the different content between prestalk cells and prespore cells(60). Mato & Marin-Cao reported that sonicated homogenate of Dictyostelium amoebae uptake ^{45}Ca depending on Mg-ATP(68). And de Chastellier & Ryter(23) reported patchilly localized Ca-ATPase at the cytoplasmic side of cell membrane. The study of uptake of ^{45}Ca by fractionated cell homogenate will elucidate Ca^{2+} sequestering system itself. Incorporated dye in a living cell may be a powerful tool to document the dynamics of intracellular free calcium ion.

cAMP is a key modulator of cell differentiation and acts as

one of potential carriers of positional information in morphorogenesis of Dictyostelium. Since chemotaxis by cAMP may produce the segregation between prestalk cells and prespore cells, it is important to study the motile machinery of cells in a slug. Separated prestalk cells move faster than prespore cells, which might result in the segregation of prestalk cells at the front of a slug and prespore cells at the tail. It is very important to compare the motile machinery of these two species of cells.

This paper described the microtubule system in Dictyostelium cells. Microtubules seemed not to change during the early development. However, it was reported that disruptors of microtubule disturbed differentiation of Dictyostelium. It is interesting how microtubules act on Dictyostelium development. The microtubules in a Dictyostelium cell are fewer than in other animal cells and have simple organization. So Dictyostelium is an excellent material for studying microtubule system. The correlation between microtubules and microfilaments in the molecular level will also be one of important problems in the light of their common possible roles of the determination of cell shape.

VI. CONCLUSION

The drastic changes in cell motile activity during the early development depend on the enlargement of the cortical microfilament system in Dictyostelium amoebae. The regional differentiation of the cortical microfilaments was shown in developing cells. The co-localization of actin and myosin in the posterior cortex in migrating cells indicated that the motive force of the amoeboid movement is produced at the tail region.

Dictyostelium myosin formed thick filaments in situ. This is the first convincing evidence for the presence of thick filaments in non-musle cells. The translocation of the filaments was observed in cells responding to chemotactic stimulation. This translocation was suggested to occur through assembly-disassembly of the filaments.

VII. ACKNOWLEDGEMENTS

I wish to express gratitude to Dr. Y. Fukui for suggesting this investigation as well as for constant guidance during the course of this work. I am greatly indebted to Prof. H. Shibaoka for his encouragement during the course of this study. I am also grateful to Prof. T. Hara for his generosity in allowing me to use the Hitachi S-430 scanning electron microscope. My special thanks are due to Dr. S. Blose of the Cold Spring Harbor Laboratory and Dr. I. Yahara of the Tokyo Metropolitan Institute of Medical Science for kindly providing monoclonal anti-tubulin antibody and rabbit anti-actin antibody, respectively. I am also grateful to Dr. H. Mori of the Fukui Prefectual College to collabolate to obtain the monoclonal anti-Dictyostelium myosin antibody. I also owe thanks to the members of the Laboratory of Cell Physiology, Faculty of Science, Osaka University.

VIII. References

1. Albrecht-Buehler, G. (1976)
Filopodia of spreading 3T3 cells. Do they have a substrate-exploring function? J. Cell Biol. 69, 275-286.

2. Albrecht-Buehler, G. (1977)
The phagokinetic tracks of 3T3 cells. Cell 11, 395-404.

3. Albrecht-Buehler, G. (1979)
The orientation of centrioles in migrating 3T3 cells. Exp. Cell Res. 120, 111-118.

4. Amato, P. A., E. R. Unaue and D. L. Taylor (1982)
Distribution of actin in spreading macrophages; comparative study on living and fixed cells. J. Cell Biol. 96, 750-761.

5. Ames, G. F. and K. Nikaido (1975)
Two-dimentional gel electrophoresis of membrane proteins. Biochemistry, 15, 616-623.

6. Bazari, W. L. and M. Clarke (1981)
Characterization of a novel calmodulin from Dictyostelium discoideum. J. Biol. Chem. 256, 3598-3603.

7. Bazari, W. L. and M. Clarke (1982)
Dictyostelium calmodulin: Production of a specific antiserum and localization in amoebae. Cell Motility 2, 471-482.

8. Bennett, H. and J. Condeelis (1984)
Decoration with myosin subfragment-1 disrupts contacts between microfilaments and the cell membrane in isolated Dictyostelium cortices. J. Cell Biol. 99, 1434-1440.

9. Bensadoum, A. and D. Weinstein (1976)
Assay of proteins in the presence of interfering materials. Anal. Biochem. 70, 241-250.

10. Bonner, J. T. (1947)
Evidence for formation of cell aggregation by chemotaxis in the development of Dictyostelium discoideum. J. Exp. Zool. 106, 1-26.

11. Bourguignon, L. Y. W., M. L. Nagpal, K. Balazovich, V. Guerriero and A. R. Means. (1982)
Association of myosin light chain kinase with lymphocyte membrane-cytoskeleton complex.

12. Brawn, S. S., K. Yamamoto and J. A. Spudich (1982)
A 40,000-dalton protein from Dictryostelium discoideum affects assembly properties of actin in a Ca^{+2}-dependent manner. J. Cell Biol. 93, 205-210.

13. Brier, J., M. Fechheimer, J. Swanson and D. L. Taylor (1983)
Abundance, relative gelation activity, and distribution of 95,000-dalton actin-binding protein from Dictyostelium discoideum. J. Cell Biol. 97, 178-185.

14. Bumann, J., B. Wurster and D. Malchow (1984)
Attractant-induced changes and oscillations of the extracellular Ca^{2+}concentration in suspensions of differentiating Dictyostelium cells. J. Cell Biol. 98, 173-178.

15. Clarke, M., G. Schatten, D. Matzia and J. A. Spudich (1976)
Visualization of actin fibers associated with the cell membrane in amoebae of Dictyostelium discoideum. Proc. Natl. Acad. Sci. USA 72, 1758-1762.

16. Clarke, M. and J. A. Spudich (1977)
Nonmuscle contractile proteins: The role of actin and myosin in cell motility and shape determination. Ann. Rev. Biochem. 46, 797-822.

17. Clarke, M., W. L. Bazari and S. C. Kayman (1980)
Isolation and properties of calumodulin from Dictyostelium discoideum. J. Bacteriol. 141, 397-400.

18. Condeelis, J. (1979)
Isolation of concanavalin A caps during various stages of formation and their association with actin and myosin. J. Cell Biol. 80, 751-758.

19. Condeelis, J. and D. L. Taylor (1977)
The contractile basis of amoeboid movement. V. The control of gelation, solation and contraction in extracts from Dictyostelium discoideum. J. Cell Biol. 74, 901-927.

20. Condeelis, J., J. Salisbury and K. Fujiwara (1981)
A new protein that gels F actin in the cell cortex of Dictyostelium discoideum. Nature 292, 161-163.

21. Condeelis, J. and M. Vahey (1982)
A calcium- and pH- regulated protein from Dictyostelium discoideum that cross-links actin filaments. J. Cell Biol. 94, 466-471.

22. Condeelis, J., M. Vahey, J. M. Carboni, J. DeMay and S. Ogihara (1984)
Properties of the 120,000- and 95,000-dalton actin-binding proteins from Dictyostelium discoideum and their possible functions in assembling the cytoplasmic matrix. J. Cell Biol. 99, 119s.

23. de Chastellie, C. and A. Ryter (1981)
Calcium-dependent deposits at the plasma membrane deposits at the plasma membrane of Dictyostelium discoideum and their possible relation with contractile proteins. Biol. Cell 40, 109-118.

24. Dinauer, M. C., S. A. Mackay and P. N. Devreotes (1980) Cyclic 3',5'-AMP relay in Dictyostelium discoideum III. The relationship of cAMP synthesis and secretion during the cAMP signalling response. J. Cell Biol. 86, 537-544.

25. Dulbecco, R., R. Allen, S. Okada and M. Bowman (1983) Functional changes of intermediate filaments in fibroblastic cells revealed by a monoclonal antibody. Proc. Natl. Acad. Sci. USA 80, 1915-1918.

26. Eckert, B. S., R. H. Warren and R. W. Rubin (1977) Structual and biochemical aspects of cell motility in amebas of Dictyostelium discoideum. J. Cell Biol. 72, 339-350.

27. Eckert, B. S. and E. Lazarides (1978) Localization of actin in Dictyostelium amebas by immunofluorescence. J. Cell Biol. 77, 714-721.

28. Engvall, E. and P. Perlman (1972) Enzyme-linked immunosorbent assay, ELIZA. III. Quantitation of specific antibodies by enzyme-labeled anti-immunoglobulin in antigen-coated tubes. J. Immunol. 109, 129-135.

29. Filosa, M. F. and Y. Fukui (1981) Dimethyl sulfoxide inhibits capping of surface receptors. Cell Biol. Int. Rep. 5, 575-579.

30. Fukui, Y. (1978) Intranuclear actin bundles induced by dimethyl sulfoxide in interphase nucleus of Dictyostelium. J. Cell Biol. 76, 146-157.

31. Fukui, Y. (1980) Formation of multinuclear cell induced by dimethyl sulfoxide: inhibition of cytokinesis and occurrence of novel nuclear divison in Dictyostelium cells. J. Cell Biol. 86, 181-189.

32. Fukui, Y. and H. Katsumaru (1980)
Dynamics of nuclear actin bundle induction by dimethyl sulfoxide and factors affecting its development. J. Cell Biol. 84, 131-140.

33. Futrelle, R. P., J. Traut and W. G. Mckee (1982)
Cell behaviour in Dictyostelium discoideum: Preaggregation response to localized cyclic AMP pulses. J. Cell Biol. 92, 807-821.

34. Galvin, N. J., D. Stockhausen, B. L. Meyers-Hutchins and W. A. Franzier (1984)
Association of the cyclic AMP chemotaxis receptor with detergent-insoluble cytoskeleton of Dictyostelium discoideum. J. Cell Biol. 98, 584-595.

35. Geller, J. and M. Brenner (1978)
The effects of 2,4-dinitrophenol on Dictyostelium discoideum oscillations. B. B. R. C. 81, 814-821.

36. Gerisch, G. and B. Hess (1974)
Cyclic-AMP-controlled oscillations in suspended Dictyostelium cells: Their relation to morphogenetic cell interaction. Proc. Natl. Acad. Sci. USA 71, 2118-2122.

37. Gerisch, G., D. Malchow, A. Huesger, V.Nanjundiah, W. Roos, U. Wick and D. Hulser (1975)
Cyclic AMP reception and cell recognition in Dictyostelium discoideum. In Developmental Biology (McMahon, D. & Fox, C. F., eds),76-88, W. A. Benjamin, Menlo Park, CA (1975)

38. Gerisch, G. and U. Wick (1975)
Intracellular oscillations and release of cyclic AMP from

Dictyostelium cells. B. B. R. C. 65, 364-370.

39. Goodloe-Holland, C. M. and E. J. Luna (1984)
A membrane cytoskeleton from *Dictyostelium discoideum* III. Plasma membrane fragments bind predominantly to the side of actin filaments. J. Cell Biol. 99, 71-78.

40. Gotlieb, A. I., L. M. May, L. Subrahmanyan and V. I. Kalnins (1981)
Distribution of microtubule organizing centers in migrating sheets of endothelial cells. J. Cell Biol. 91, 589-594.

41. Greenberg Giffard, R., J. A. Spudich and A. Spudich (1983)
Ca^{2+}-sensitive isolation of a cortical actin matrix from *Dictyostelium* amoebae. J. Musc. Cell Motility 4, 115-131.

42. Hellewell, S. B. and D. L. Taylor (1979)
The contractile basis of amoeboid movement. VI. The solation-contraction coupling hypothesis. J. Cell Biol. 83, 633-648.

43. Herman, I. M., N. J. Crisona and T. D. Pollard (1981)
Relation between cell activity and the distribution of cytoplasmic actin and myosin. J. Cell Biol. 90, 84-91.

44. Herman, I. M. and T. D. Pollard (1981)
Electron microscopic localization of cytoplasmic myosin with ferritin-labeled antibodies. J. Cell Biol. 88, 346-351.

45. Hirokawa,N., L. G. Tilney, K. Fujiwara and J. E. Heuser (1982)
Organization of actin, myosin and intermediate filaments in the brush border of intestinal epithelial cells. J. Cell Biol. 94, 425-443.

46. Huxley, H. E. (1969)
The mechanism of muscular contraction. Science 164, 1356-1366.

47. Jacobson, B. S. (1980)
Actin binding to the cytoplasmic surface of the plasma membrane isolated from Dictyostelium discoideum. Biochem. Biophys. Res.

48. Johnson, G. D. and G. de C. Nogueira Aranjo (1981)
A simple method of reducing the fading of immunofluorescence during microscopy. J. Immunol. Methods 43, 349-350.

49. Juliani, M. H. and C. Klein (1977)
Calcium ion effects on cyclic adenosine 3':5'-monophosphate bindings to the plasma membrane of Dictyostelium discoideum. B. B. A. 497, 369-376.

50. Kamiya, N. and K. Kuroda (1965)
Movement of the myxomycete plasmodium. I. A study of glycelinated models. Proc. Japan. Acad. 41, 837-841.

51. Kitanishi, T., H. Shibaoka and Y. Fukui (1984)
Distribution of microtubules and retardation of development of Dictyostelium with ethyl-N-phenylcarbamate and thiabendazole. Protoplasma 120, 185-196.

52. Koonce, M. P., R. A. Cloney and M. W. Berns (1984)
Laser irradiation of centrosomes in Newt eosinophiles: Evidence of centriole role in motility. J. Cell Biol. 98, 1999-2010.

53. Kuczmarski, E. R. and J. A. Spudich (1980)
Regulation of myosin self-assembly: Phosphorylation of Dictyostestelium heavy chain inhibits formation of thick filaments. Proc. Natl. Acad. Sci. U.S.A. 77, 7292-7296.

54. Kuriyama, R., C. Sato, Y. Fukui and S. Nishibayashi (1982)
In vitro nucleation of microtubules from microtubule-organizing center prepared from cellular slime mold. Cell Motil. 3. 257-

272.

55. Laemmli, U. K. (1970)
Cleavage of structural proteins during the assembly of the head of bacteriophages T4. Nature (Lond.) 227, 680-685.

56. Lowry, O. H., N. Rosebrough, A. L. Farr and R. J. Randall (1951)
Protein measurement with Folin phenol reagent. J. Biol. Chem. 193, 265-275.

57. Luna, E. J., C. M. Goodloe-Holland and H. M. Ingalls (1984)
A membrane cytoskeleton from Dictyostelium discoideum. II. Integral proteins mediate the binding of plasma membrane to F-actin affinity beads. J. Cell Biol. 99, 58-70.

58. Luna, E. J., V. M. Fowler, J. Swanson, D. Brawn and D. L. Taylor (1981)
A membrane cytoskeleton from Dictyostelium discoideum. I. Identification and partial characterrization of actin-binding activity. J. Cell Biol. 88, 396-409.

59. Luna, E. J., Y.-L. Wang, E. W. Voss, Jr., D. Branton and D. L. Taylor (1982)
A stable, high capacity, F-actin affinity column. J. Biol. Chem. 257, 13095-13100.

60. Maeda, Y. and M. Maeda (1973)
The calcium content of the cellular slime mold, Dictyostelium discoideum, during development and differentiation. Exp. Cell Res. 82, 125-130.

61. Malchow, D., R. Böhme and H. J. Rahmsdorf (1981)
Regulation of phosphorylation of myosin heavy chain during the chemotactic response of Dictyostelium cells. Eur. J. Biochem.

117, 213-218.

62. Malchow, D., R. Böhme and U. Gras (1982)
On the role of calcium in chemotaxis and oscillation of Dictyostelium cells. Biophysics of Structure and Mechanism 9, 131-136.

63. Malchow, D., V. Nanjundah and G. Gerisch (1978)
PH oscillation in cell suspensions of Dictyostelium discoideum: Their relation to cyclic-AMP signals. J. Cell Sci. 30, 319-330.

64. Malech, H. L., R. K. Root and J. I Gallin (1977)
Structual analysis of human neutrophil migration. Centriole, microtubule and microfilament orientation and function during chemotaxis. J. Cell Biol. 75, 666-693.

65. Margolskee, J. P. and H. F. Lodish (1980)
The regulation of the synthesis of actin and two other proteins induced early in Dictyostelium discoideum development. Dev. Biol. 74, 50-64.

66. Maruta, H., W. Baltes, P. Dieter, D. Marme and G. Gerisch (1983)
Myosin heavy chain kinase inactivated by Ca^{2+}/calmodulin from aggregation cells of Dictyostelium discoideum. The EMBO Journal 2, 535-542.

67. Mast, S. O. (1926)
Structure, movement, locomotion and stimulation in Amoeba.

68. Mato, J. M. and D. Marin-Cao (1979)
Protein and phospholipid methylation during chemotaxis in Dictyostelium discoideum and its relationship to calcium movements. Proc. Natl. Acad. Sci. USA 76, 6106-6109.

69. McRobbie, S. J. and P. C. Newell (1983)

Changes in actin associated with the cytoskeleton following chemotactic stimulation of Dictyostelium discoideum. B. B. R. C. 115, 351-359.

70. Mcrobbie, S. J. and P. C. Newell (1984) A new model for chemotactic signal transduction in Dictyostelium discoideum. B. B. R. C. 123, 1076-1083.

71. Macrobbie, S. J. and P. C. Newell (1984) Chemoattractant-mediated changes in cytoskeletal actin of cellular slime molds. J. Cell Biol. 68, 139-151.

72. Nachmias, V. T. (1964) Fiblillar structures in the cytoplasm of Chaos chaos. J. Cell Biol. 23, 183-188.

73. Naib-majani, W., W. Stockem and K. E. Wohlfarth-Bottermann (1982) Immunocytochemistry of the acellular slime mold Physarum polycephalum. II. Spacial organization of cytoplasmic actin. Eur. J. Cell Biol. 24, 103-114.

74. Niederman, R. and T. D. Pollard (1975) Human platelelt myosin. II. In vitro assembly and structure of myosin filaments. J. Cell Biol. 67, 72-92.

75. O'Farrell, P. H. (1975) High resolution two-dimensional electrophoresis of proteins. J. Biol. Chem. 250, 4007-4021.

76. Pan, P., E. M. Hall and J. T. Bonner (1972) Folic acid as second chemotactic substance in the cellular slime molds. Nature New Biol 237, 181-182.

77. Peltz, G., E. R. Kuczmarski and J. A. Spudich (1981) Dictyostelium myosin: Characterization of chymotryptic fragments

and localization of the heavy chain phosphorylation site. J. Cell Biol. 89, 104-108.

78. Pollard, T. D. and S. Ito (1970)
Cytoplasmic filaments of Amoeba proteus. I. The role of filaments in consistency changes and movement. J. Cell Biol. 46, 267-289.

79. Potel, M. J. and S. A. Mackay (1979)
Preaggregation cell motion in Dictyostelium. J. Cell Sci. 36, 281-309.

80. Rodriguez, J. and F. Deinhardt (1960)
Preparation of a semipermanent mounting medium for fluorescent antibody studies. Virology. 12, 316-317.

81. Roos, U. -P. (1975)
Mitosis in the cellular slime mols Polysphondylium violaceum. J. Cell Biol. 64, 480-491.

82. Roos, W., C. Scheidegger and G. Gerisch (1977)
Adenylate cyclase activity oscillations as signals for cell aggregation in Dictyostelium discoideum. Nature 266, 259-261.

83. Rubino, S., M. Fighetti, E. Unger and P. Cappuccinelli (1984)
Localization of actin, myosin and microtubular structures during directional locomotion of Dictyostelium amoebae. J. Cell Biol. 98, 382-390.

84. Rubino, S., E. Unger, G. Fogu and P. Cappuccinelli (1982)
Effect of microtubule inhibitors on the tubulin system in Dictyostelium discoideum. Zeitschrift fur Allgemeine Mikrobiologie 22, 127-131.

85. Saito, M. (1979)

Effect of extracellular Ca^{2+} on the morphogenesis of Dictyostelium discoideum. Exp. Cell Res. 123, 79-86.

86. Samuel, E. W. (1961)
Orientation and rate of locomotion of individual amoebas in the life cycle of cellular slime mold Dictyostelium mucoroides. Develop. Biol. 3, 317-335.

87. Sanger, J. M. and J. W. Sanger (1980)
Banding and polality of actin filaments in interphase and cleaving cells. J. Cell Biol. 86, 568-575.

88. Schroedor, T. E. (1973)
Actin in dividing cells: Contractile ring filaments bind heavy meromyosin. Proc. Natl. Acad. Sci. USA 70, 1688-1692.

89. Shaffer, B. M. (1964)
Intracellular movement and locomotion of cellular slime mold amoebae. In 'Primitive Motile Systems in Cell Biology', 387-405 (R. D. Allen & N, Kamiya eds.) Academic Press, New York.

90. Sholey, J. M., K. A. Taylor and J. Kendrick-Jones (1980)
Regulation of non-muscle myosin assembly by calmodulin-dependent light chain kinase. Nature 287, 233-235.

91. Shulman, M., C. D. Wilde and G. Kohler (1978)
A better cell line for making hybridomas secreting specific antibodies. Nature 276, 269-270.

92. Spudich, A. and J. A. Spudich (1979)
Actin in Triton-treated cortical preparations of unfertilized and fertilized sea urchin eggs. J. Cell Biol. 82, 212-226.

93. Spudich, J. A. (1974)
Biochemical and structual studies of actomyosin-like proteins from non-muscle cells. J. Biol. Chem. 249, 6013-6020.

94. Stockem, W., H. U. Hoffmann and W. Gawlitta (1982)
Spatial organization and fine structure of the cortical filament layer in normal locomoting Amoeba proteus.

95. Stockem, W., W. Naib-Majani and K. E. Wohlfarth-Bottermann (1983)
Pinocytosis and locomotion of amoebae. XIX. Immunocytochemical demonstration of actin and myosin in Amoeba proteus.
Eurp. J. Cell Biol. 29, 171-178.

96. Swanson, J. A. and D. L. Taylor (1982)
Local and spatially coordinated movements in Dictyostelium discoideum amoebae during chemotaxis. Cell 28, 225-232.

97. Taylor, D. L. (1977)
The contractile basis of amoeboid movement. IV. The viscoelasticity and contractility of Amoeba cytoplasm in vitro.
Exp. Cell Biol. 105, 413-426.

98. Taylor, D. L., J. Rhodes and S. Hammond (1976)
The contractile basis of amoeboid movement. II. Structure and contractility of motile extracts and plasmalemma-ectoplasm ghost.
J. Cell Biol. 70, 123-143.

99. Taylor, D. L., J. R. Blinks and G. Reynolds (1980)
Contractile basis of amoeboid movement. VII. Aequorin luminescence during amoeboid movement, endocytosis and capping.
J. Cell Biol. 86, 599-607.

100. Taylor, D. L. and J. A. Condeelis (1979)
Cytoplasmic structure and contractility in amoeboid cells.
Int. Rev. Cytol. 56, 57-144.

101. Tomchik, K. J. and P. N. Devreotes (1981)
Adenosine 3',5'-monophsphate waves in Dictyostelium discoideum:

A demonstration by isotope dilution-fluorography. Science 212, 443-446.

102. Towbin, H., T. Staehelin and J. Gordon (1979) Electrophoretic transfer of proteins from polyacrylamide gels to nitrocellulose sheets: Procedure and some applications. Proc. Natl. Acad. Sci. USA 76, 4350-4354.

103. Uyemura, D. G., S. S. Brawn and J. A. Spudich (1978) Biochemical and structual characterization of actin from Dictyostelium discoideum. J. Biol. Chem. 253, 9088-9096.

104. Valerius, N., O. Stendahl, J. Hartwig and T. Stossel (1981) Distribution of actin-binding protein and myosin in polymorphonuclear leukocytes during locomotion and phagocytosis. Cell 24, 195-202.

105. Van Haastert, P. J. M., R. J. W. DeWit and T. M. Konijn (1982) Antagonists of chemoattractants reveal separate receptors for cAMP, folic acid and pterin in Dictyostelium. Exp. Cell Res. 140, 453-456.

106. Varnum, B. and D. R. Soll (1984) Effects of cAMP on single cell motility in Dictyostelium. J. Cell Biol. 99, 1151-1155.

107. Watts, D. J. and J. A. Ashworth (1970) Growth of myxamoebae of the cellular slime mold Dictyostelium discoideum in axenic culture. Biochem. J. 119, 171-174.

108. White, E., E. M. Tolbert and E. R. Katz (1983) Identification of tubulin in Dictyostelium discoideum: Characterization of some unique properties. J. Cell Biol. 97, 1011-1019.

109. Willingham, M. C., S. S. Yamada, P. J. Bechtel, A. V. Rutherford and I. H. Pastan (1981)
Ultrastructual immunocytochemical localization of myosin in cultured fibroblastic cells. J. Histchem. Cytochem. 11, 1289-1301.

110. Woolley, D. E. (1972)
An actin-like proteins from amoebae of Dictyostelium discoideum Arch. Biochem. Biophys. 150, 519-530.

111. Yamamoto, K., J. D. Pardee, J. Recdler, L. Stryer and J. A. Spudich. (1982)
Mechanism of interaction of Dictyostelium Severin with actin filaments. J. Cell Biol. 95, 711-719.

112. Yumura, S. and Y. Fukui (1983)
Filopodelike projections induced with dimethyl sulfoxide and their relevance to cellular polarity in Dictyostelium.
J. Cell Biol. 96, 857-865.

113. Yumura, S., H. Mori and Y. Fukui (1984)
Localization of actin and myosin for the study of amoeboid movement in Dictyostelium using improved immunofluorescence.
J. Cell Biol. 99, 894-901.

114. Yumura, S. and Y. Fukui (1985)
Myosin thick filaments in Dictyostelium and a reversible change in distribution in response to cAMP. Nature, in press.

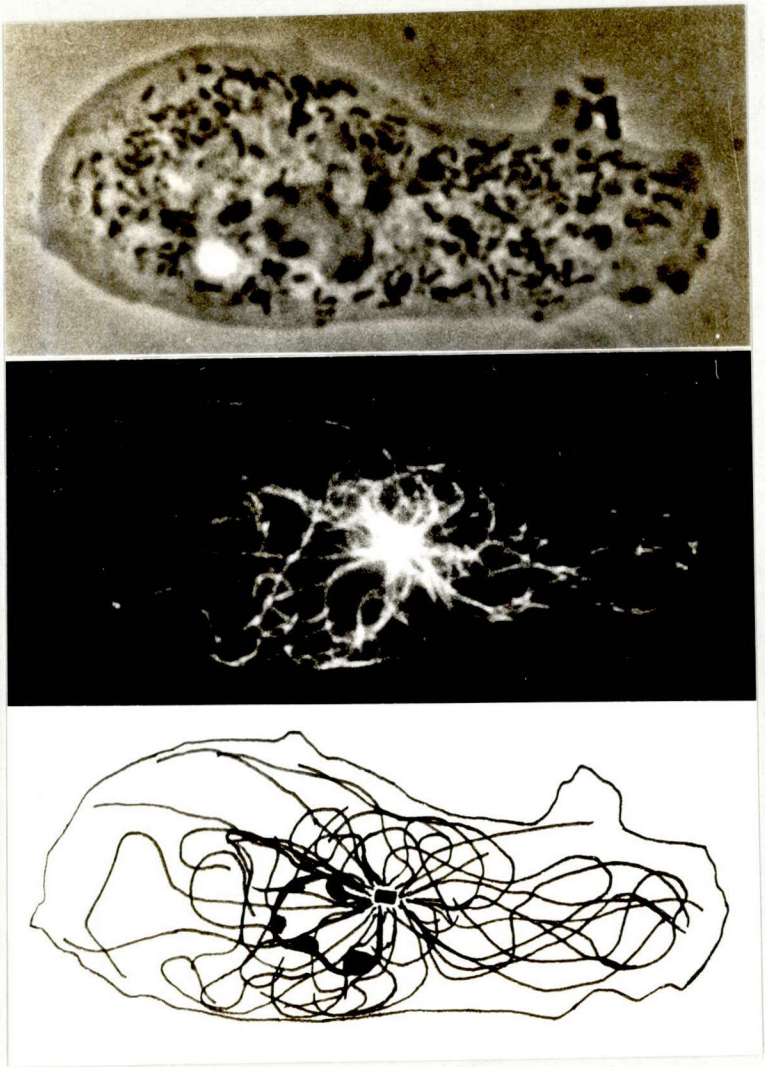

Fig. 1. A typical immunofluorescence of a locomotory Dictyostelium discoideum amoeba using monoclonal anti-tubulin. The top figure is a phase-contrast micrograph of a fixed cell by agar-overlay technique. The same cell was stained with monoclonal anti-tubulin (the middle) and microtubules, MTOC, the contours of the cell were traced (the bottom).

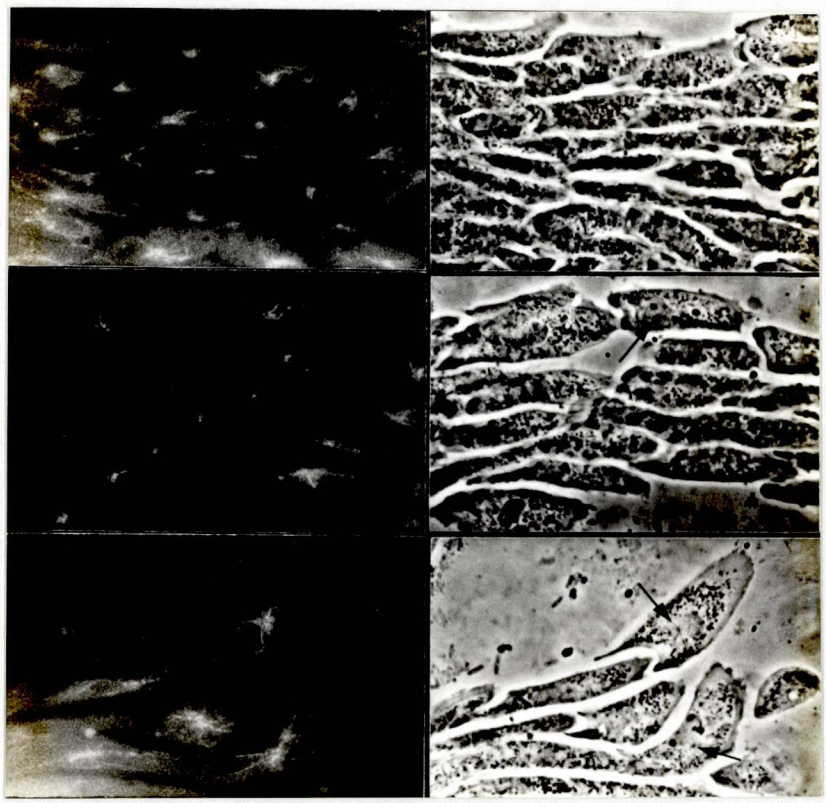

Fig. 2. Immunofluorescence micrographs of aggregating cells in the aggregation stream stained with anti-tubulin. The direction of cell migration is from the right to the left.

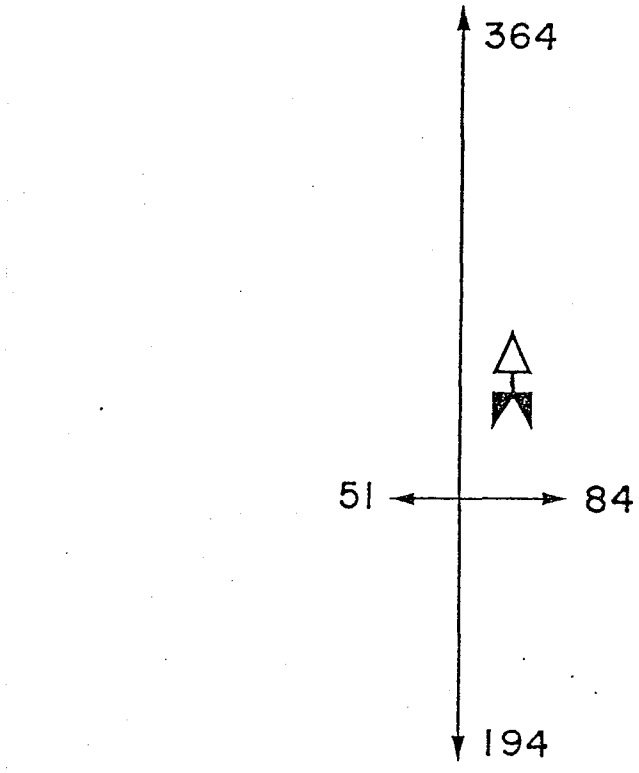

Fig. 3. The diagram showing the frequency of the position of MTOC with reference to that of nucleus. A total of 693 cells was investigated, and the Student t test ($p < 0.01$) indicated that the positioning of the MTOC in the anterior side of the nucleus was very significant. Arrow indicates the direction of cell migration.

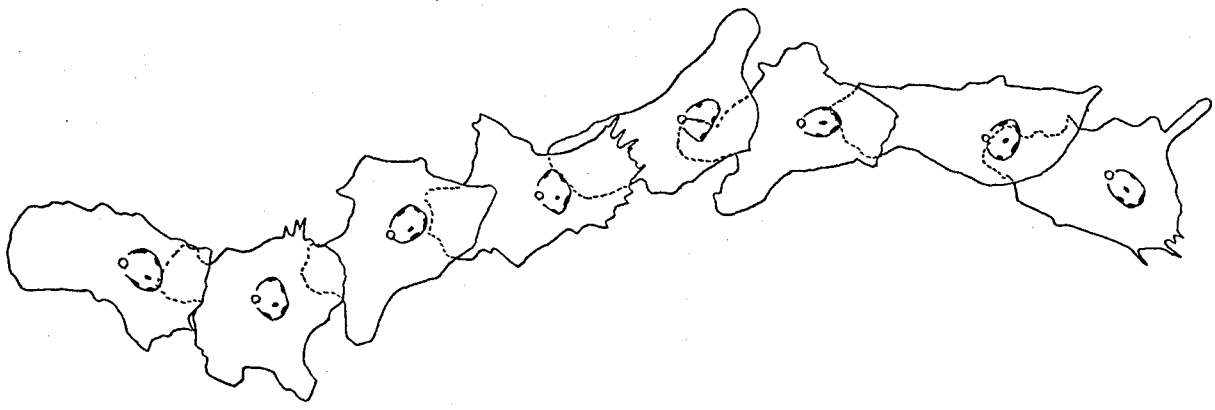

Fig. 4. The traces of MTOC and nucleus in a locomoting cell. By taking photographs of a locomoting cell every 30 sec, the location of MTOC and nucleus was traced. MTOC was always located in front of the nucleus.

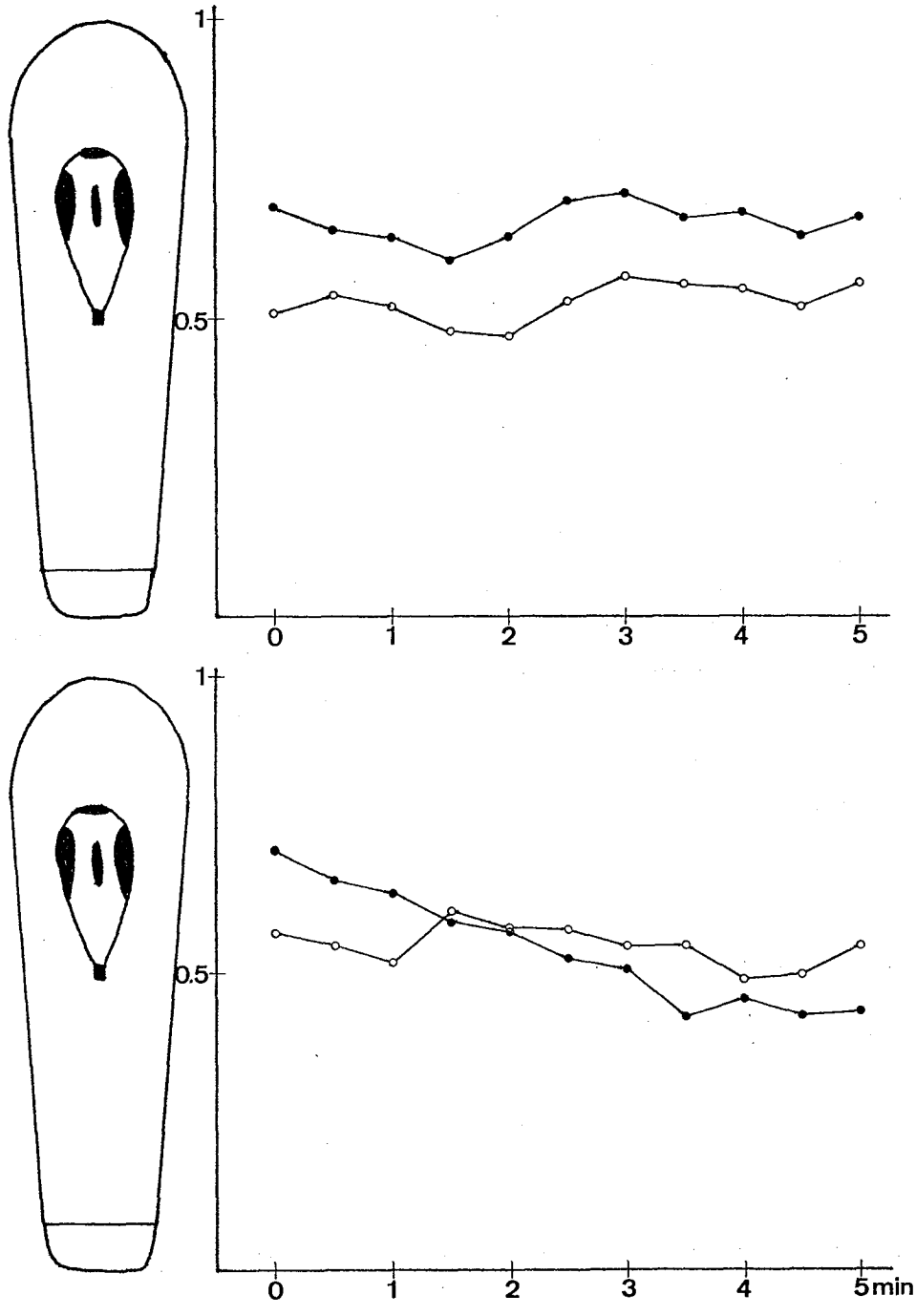

Fig. 5. The location of MTOC and nucleus in locomoting cells. Two examples of taces performed as in Fig. 4. The parameter (ordinate, p value) was obtained by dividing the distance from the anterior end of the cell to the location of MTOC (open circles) or nucleus (filled circles) by the longitudial length of the cell. MTOC's were always located at the middle portion of the cell even in such case that MTOC changed the location to opposite side of the nucleus (bottom figure).

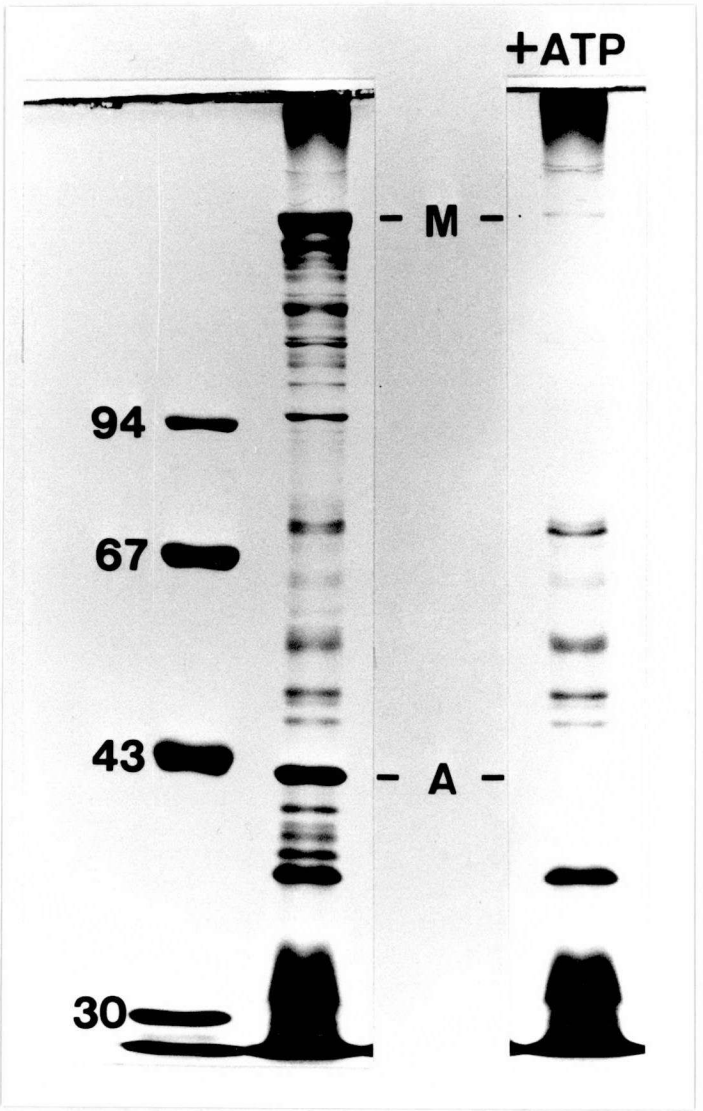

Fig. 6. SDS PAGE of isolated cell membrane fractions and the dissociation of actin and myosin from the membrane treated with ATP. The membrane fractions were prepared according to Spudich, treated with preparation buffer containing 1 mM Mg-ATP, centrifuged at 10,000 rpm and solubilized in SDS sample buffer. A, actin ; M, myosin heavy chain. The left numbers are molecular weights (k dalton) of marker proteins.

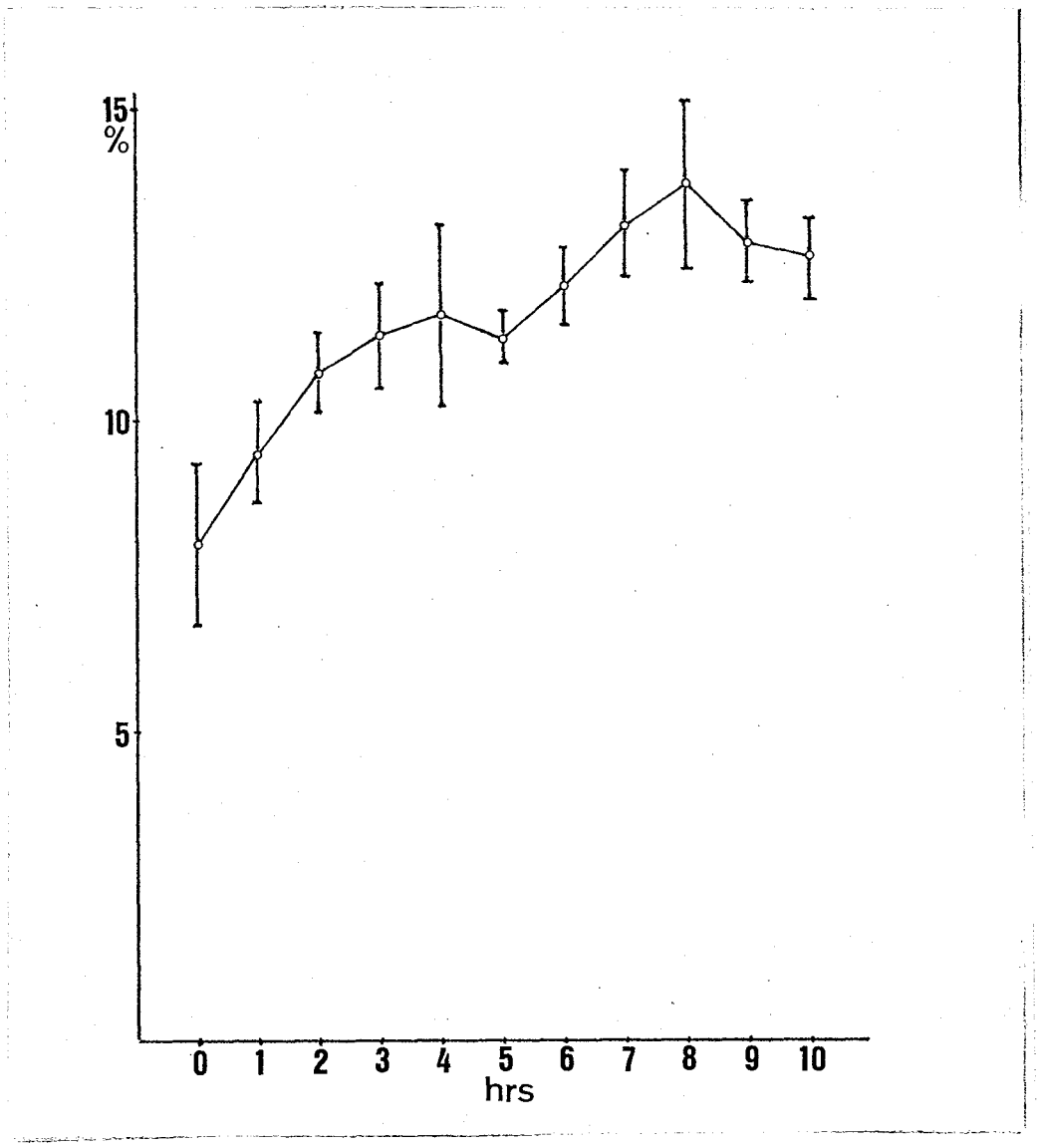

Fig. 7. The changes in the relative protein content of Triton-insoluble ghosts during the early development of Dictyostelium. An aliquot of pellet of amoebae (AX-2) in each developmental phase was permeabilized with 0.5% Triton-X 100 in P-buffer and centrifuged at 10,000 rpm. The protein content ofthe Triton-insoluble ghosts was divided by the whole cell's proteincontent. Each values (open circles) were calculated from at least 4 experiments. Bars represent standard deviations of these values. Ordinate: relative protein content of Triton-insoluble ghosts, abcissa: time (hours) after the starvation.

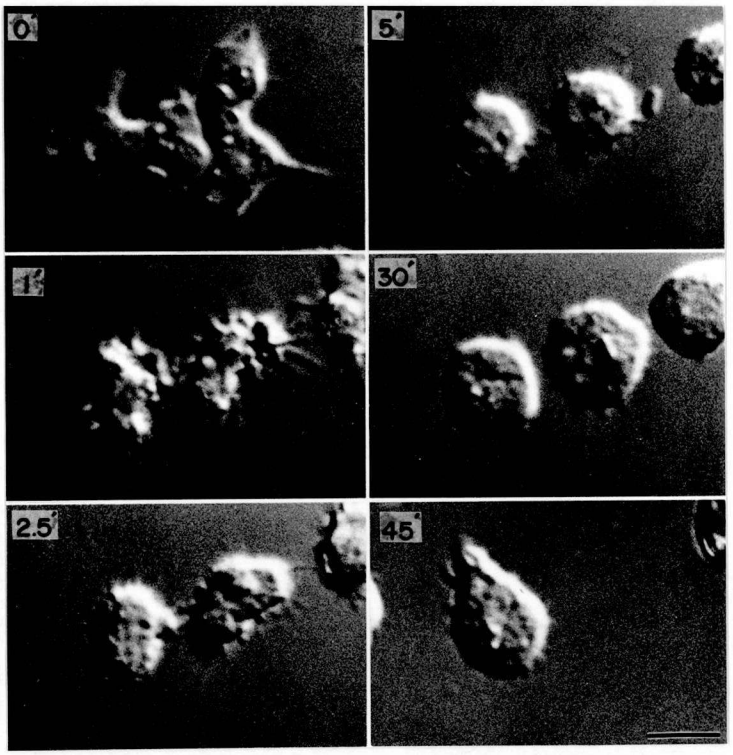

Fig. 8. Differential interference micrographs showing the sequential changes in the morphorogy of Dictyostelium mucoroides cells treated with 5% DMSO (same micrographic field). Note that thin projections formed immediately after the treatment and these projections reduced in length at the same time with the rounding-up of the cells. In 20-30 min, the cells resumed the cytoplasmic streaming and locomotion and started to migrate forming a pseudopode.

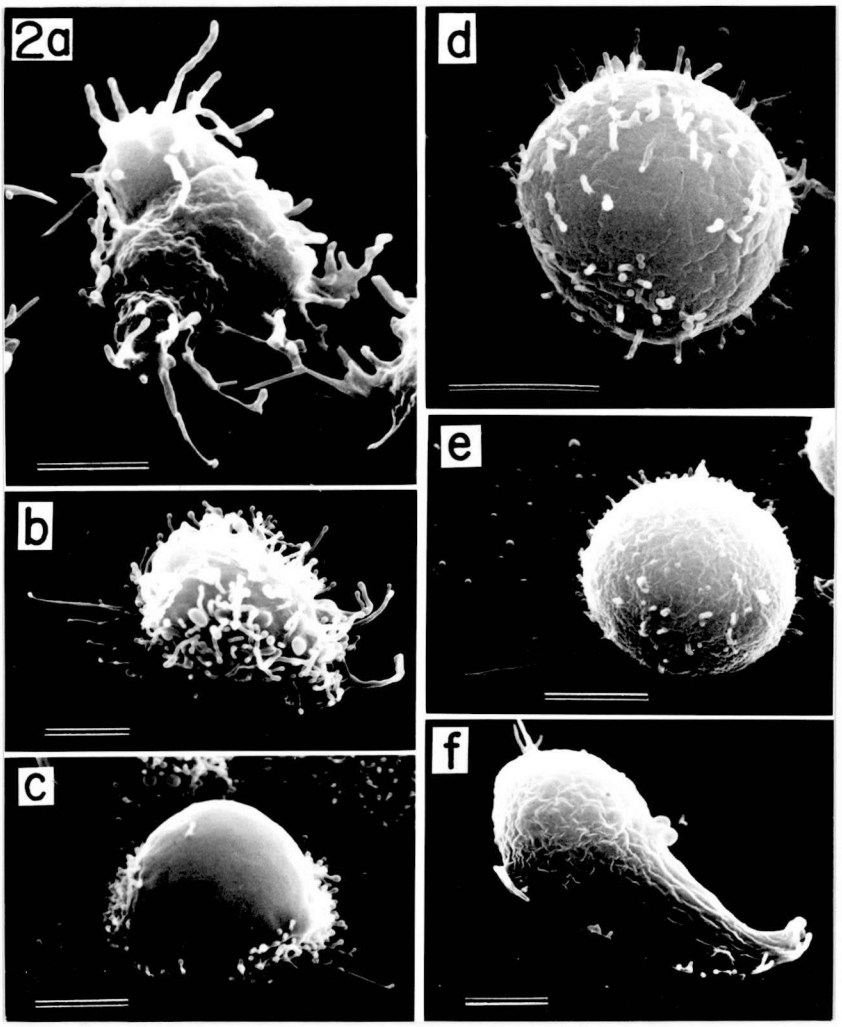

Fig. 9. Scanning electron micrographs showing the surface architecture of D. mucoroides cells treated with 5% DMSO. (a) A control cell on the plastic substratum, extending several to tens of long filopodia. (b) A cell treated for 2.5 min, showing numerous thin projections as well as a few blebs. (c) The cell treated for 5 min, showing the smooth architecture of the surface and the decrease in length of the projections. (d) A cell treated for 10 min, showing the rounding-up of the overall morphology and the decrease in length and number of the projections. (e) A cell 30 min after the treatment,showing that most projections had disappeared, and the surface displayed a wrinkled texture again. (f) A cell treated for 60 min. It extended a pseudopode and apparently started to migrate. Bar, 2.5 μm. Tilt angle: a,b,c,e and f; 60°. d,45°.

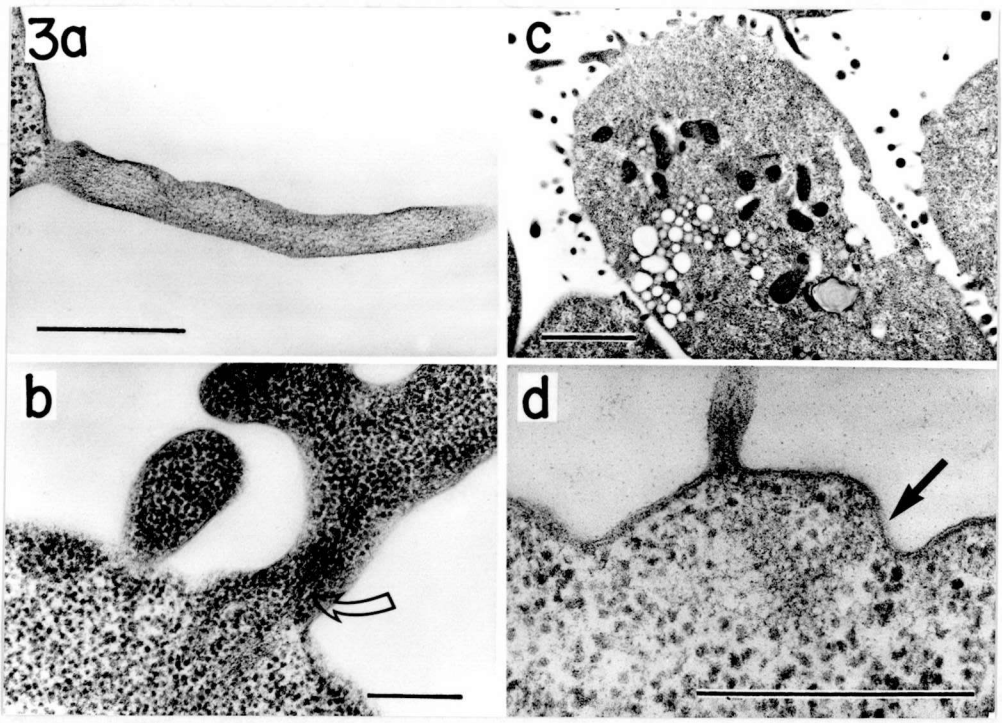

Fig. 10. Transmission electron micrographs showing the fine structure of surface projections of control and DMSO-treated cells. (a) A filopodium of a control cell, showing arrays of microfilaments inside of it. (b) The DMSO-induced projections of the cell treated with 5% DMSO for 5 min. Note that the microfilaments, as well as numerous ribosomes, were involved in the projections (arrow). (c) A low magnification micrograph of the cells treated with 5% DMSO for 5 mim, showing many projections with high electron density formed on the surface. (d) A high magnification micrograph of the cortex layer of the cell treated for 30 min. Note that the cortex microfilaments returned to their location just beneath the plasma membrane and were apparently associated with the concavities of the membrane (arrow). Bar, (a,b and d) 0.5 μm. Bar (c), 2 μm.

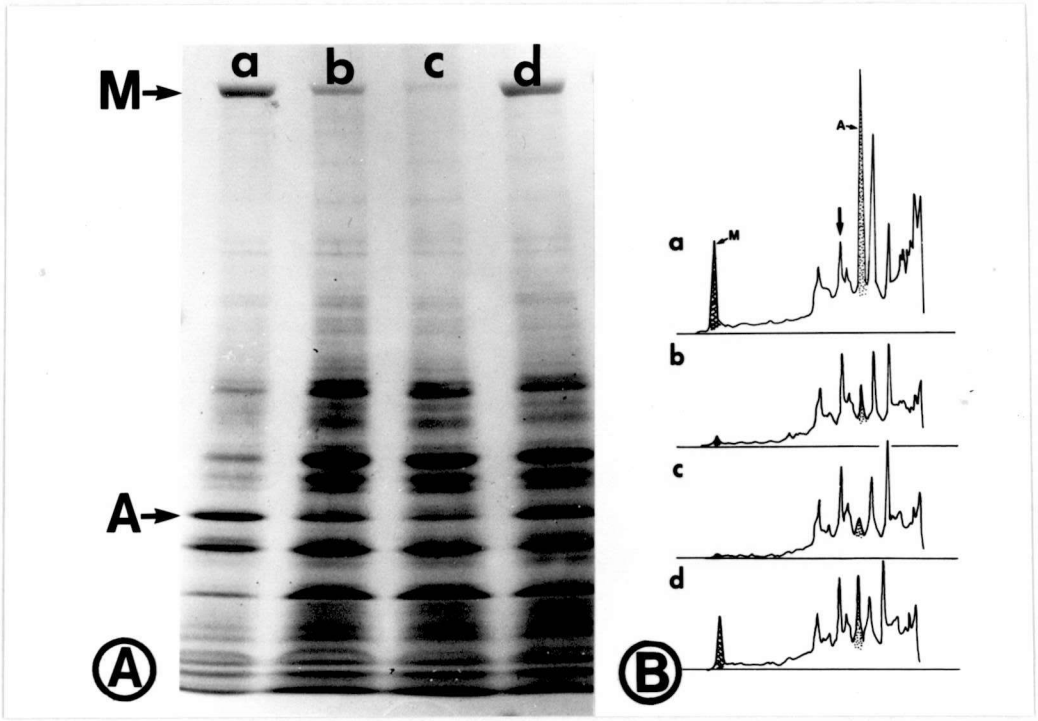

Fig. 11. SDS PAGE of Dictyostelium membrane fractions. [A] The membrane fractions were prepared according to Spudich, followed by the SDS PAGE on 5-15% linear gradient gels containing 0.1% SDS. 50 ug of the proteins was charged on each slot. The membrane were isolated from cells treated with 5% DMSO for (a) 0 min, (b) 5 min, (c) 15 min and (d) 30 min. A, actin; M, myosin heavy chain. [B] The densitometry traces of the gels in panel A, which were standarized by the surface glycoprotein peak (arrow). a-d represent the traces of the gels a-d in [A].

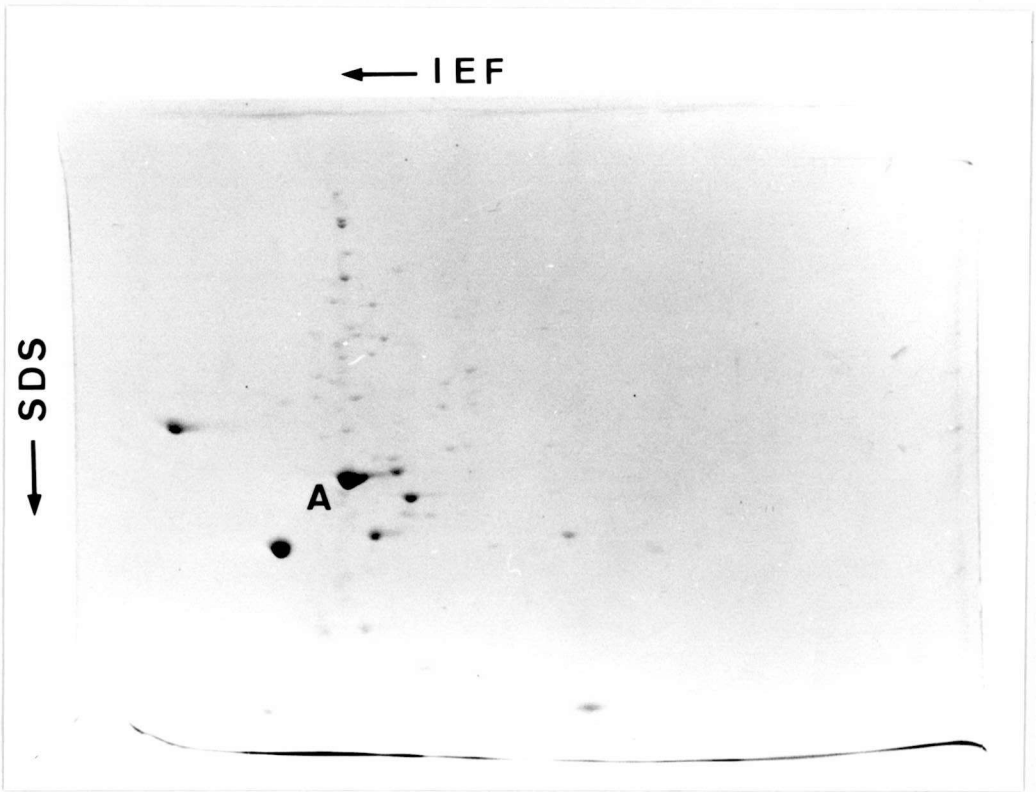

Fig. 12. Two dimensional gel electrophoresis of the membrane fraction from Dictyostelium cells. The membrane was solubilized with 1% SDS and analyzed by two dimensional electrophresis according to O'Farrell. The major spot (A) had an isoelectric point of 5.6 and a mobility identical to that of the 42 kdalton protein, indicating that it was actin.

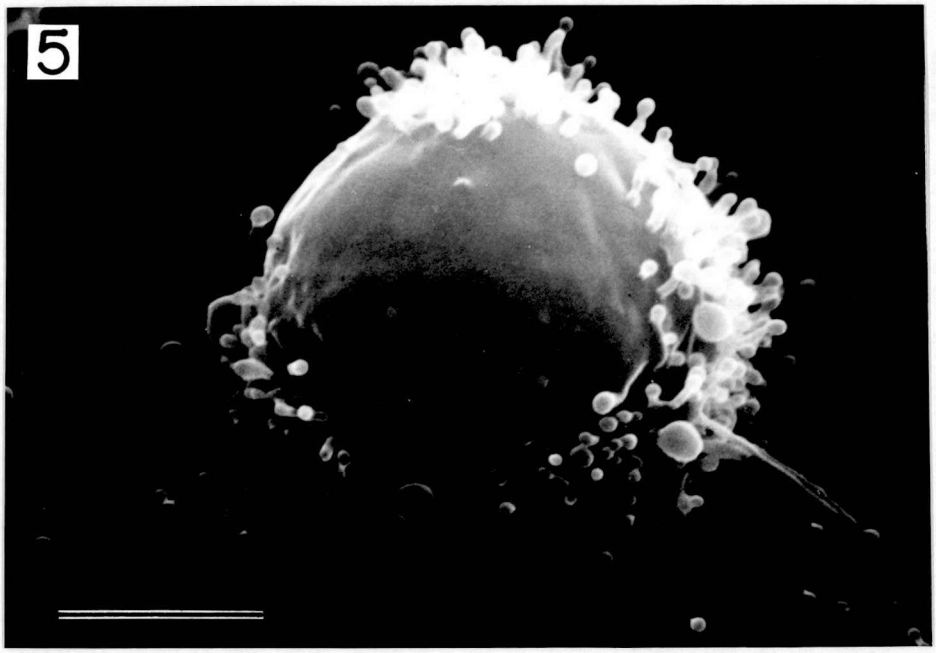

Fig. 13. A scanning electron micrograph of a cell treated with 5% DMSO for 5 min. Note that the filopodelike projections were induced to form on a restricted region of the cell surface. It is also noteworthy that the surface architecture is very smooth on the portion excluded from the projections. Bar, 2.5 μm.

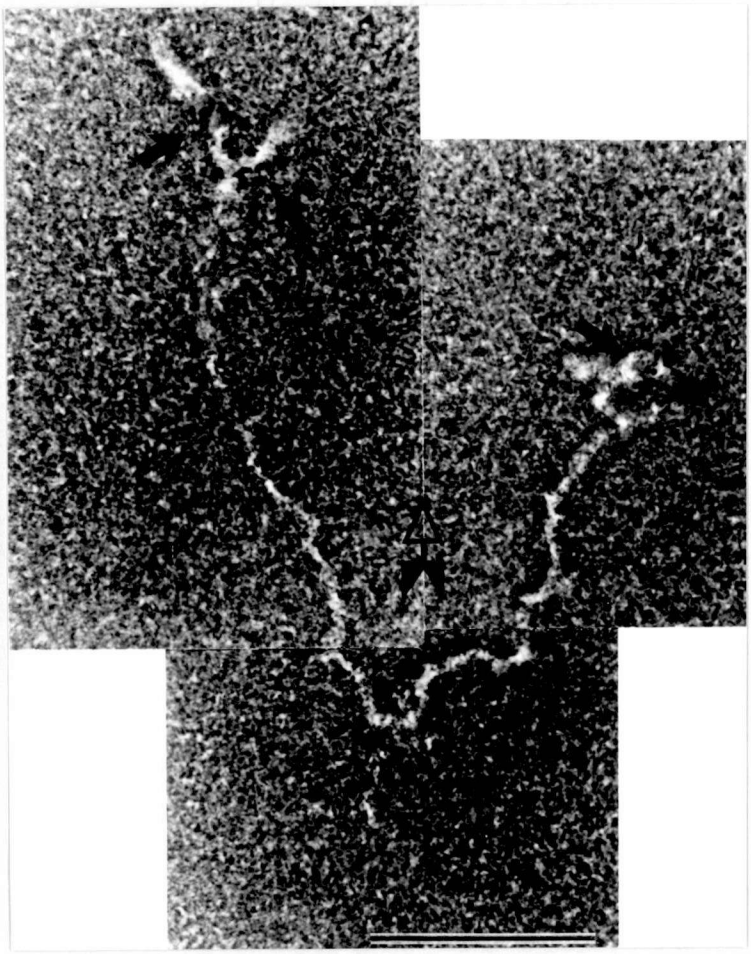

Fig. 14. The phagokinetic tracks of Dictyostelium cells. A composite phase-contrast micrograph showing a branched track representing two successive cytokinesis, of producing four daughter cells (small arrows). The large arrow indicates the direction of the movement of the cells. Bar, 50 μm.

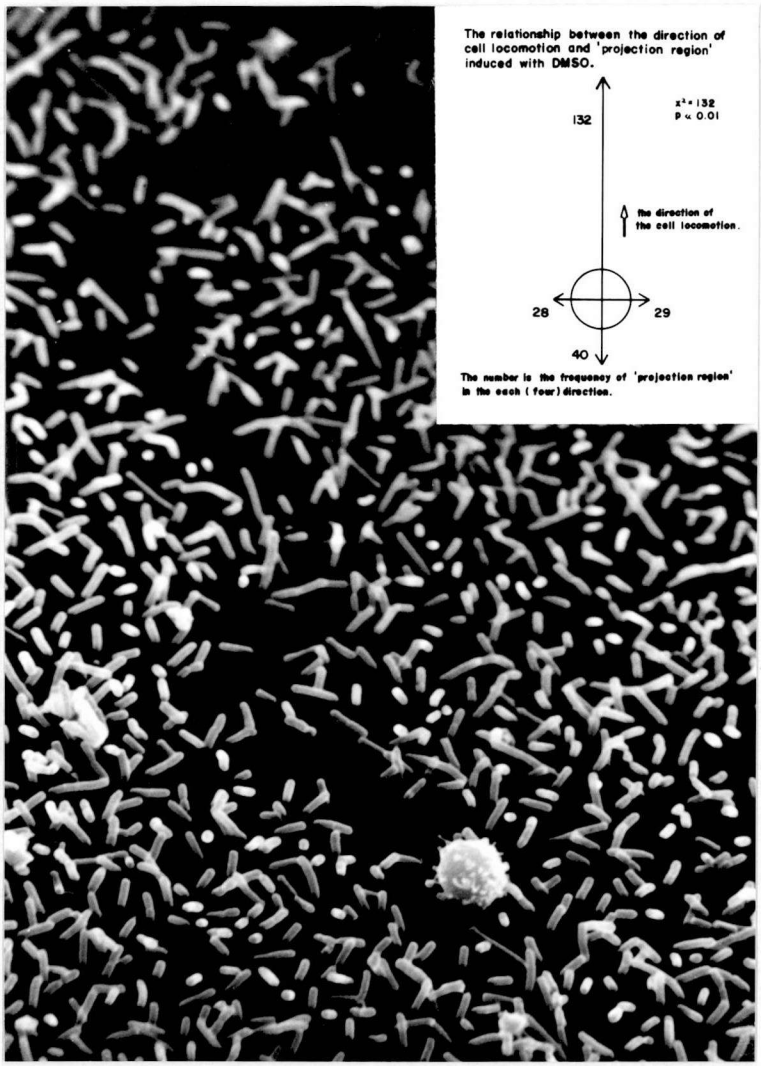

Fig. 15. A scanning electron micrograph of a migrating cell treated with 5% DMSO for 5 min subsequent to the formation of the phagokinetic track. It is apparent that the projections were primarily induced to form on the anterior end of the cell. Inset: The diagram showing the frequency of the formation of the DMSO-induced projection regions with reference to the direction of cell locomotion. The frequency was estimated according to the SEM observations. The large arrow indicates the direction of cell migration and the numbers represent the frequency at which the DMSO-induced projection regions formed on each side of the cells. The Student t test shows that the probability of the formation of the projection region at the anterior end ofthe cells is significant ($P < 0.01$).

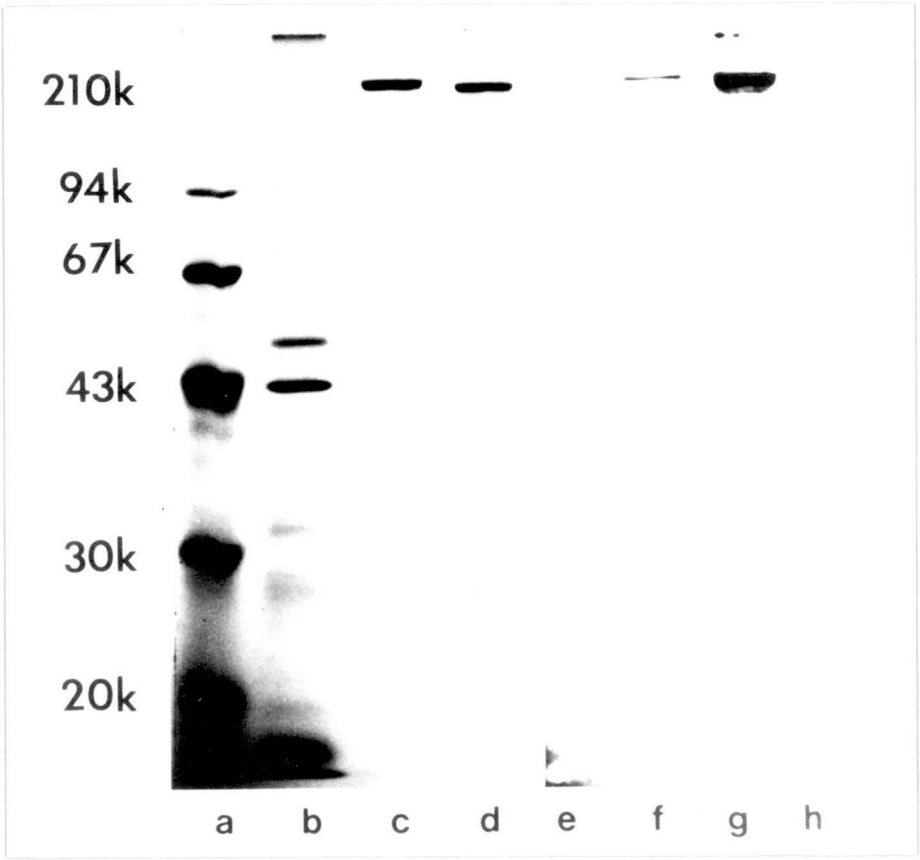

Fig. 16. Western blot of the monoclonal anti-Dictyostelium myosin (DM-2) antibody. The samples were electrophoresed on 10% SDS PAGE and stained with Coomasie blue (a-d) or after blotting to nitrocellulose paper, labeled with peroxidase-labeled anti-mouse IgG subsequent to the incubation with DM-2 (e-h). Slot (a, e): molecular weight markers, (b, f): Dictyostelium cell lysate (25 μg), (c, g): Dictyostelium myosin (5 μg), (d,h): rabbit skeletal muscle myosin (5 μg). DM-2 specifically bound to the heavy chain of Dictyostelium myosin (f, g) but neither to rabbit skeletal (d, h) nor chiken gizzard smooth muscle myosin (210k band in a,e).

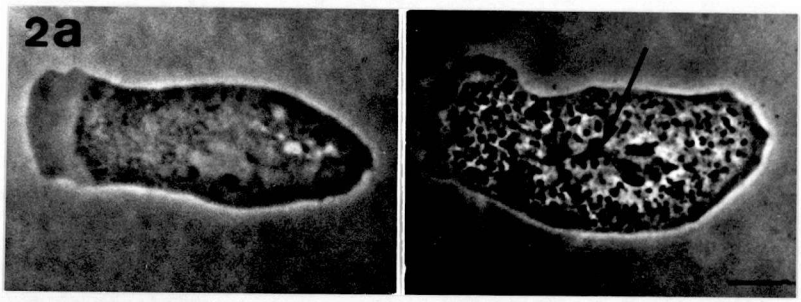

Fig. 17. Comparative phase-contrast microscopy of Dictyostelium amoebae before (a) and after (b) fixation by the agar-overlay technique. Cell structure was well preserved and the arrow indicates the site of the nuclear-associated body (MTOC). Bars, 5 μm.

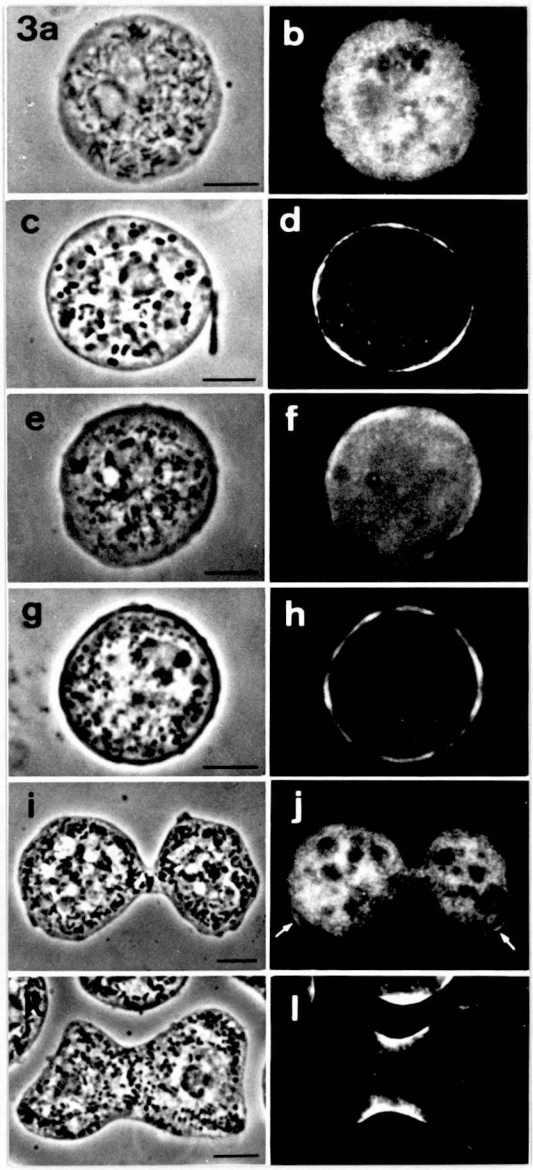

Fig. 18. Indirect immunofluorescence of vegetative Dictyostelium amoebae prepared by the agar-ovelay technique showing the distribution of actin and myosin. (a, b) A vegetative amoeba stained with anti-actin showing diffuse fluorescence in the cytoplasm. (c, d) A vegetative amoeba stained with monoclonal anti-myosin (DM-2) showing peripheral staining. (e, f) A round cell, which was allowed to develop for 2 hrs on agar plate, then fixed and stained with anti-actin. Peripheral staining became evident by 2 hrs of incubation. (g, h) A round cell like that of (e), stained with DM-2 and showing peripheral staining. (i,j) A dividing (telophase) cell stained with anti-actin. Note the staining of pollar small pseudopodes (arrows). (k, l) A dividing cell staining at the cleavage furrow. The staining pattern suggests that the filamentous structure is aligned to the axis of constriction. Bar, 5 μm.

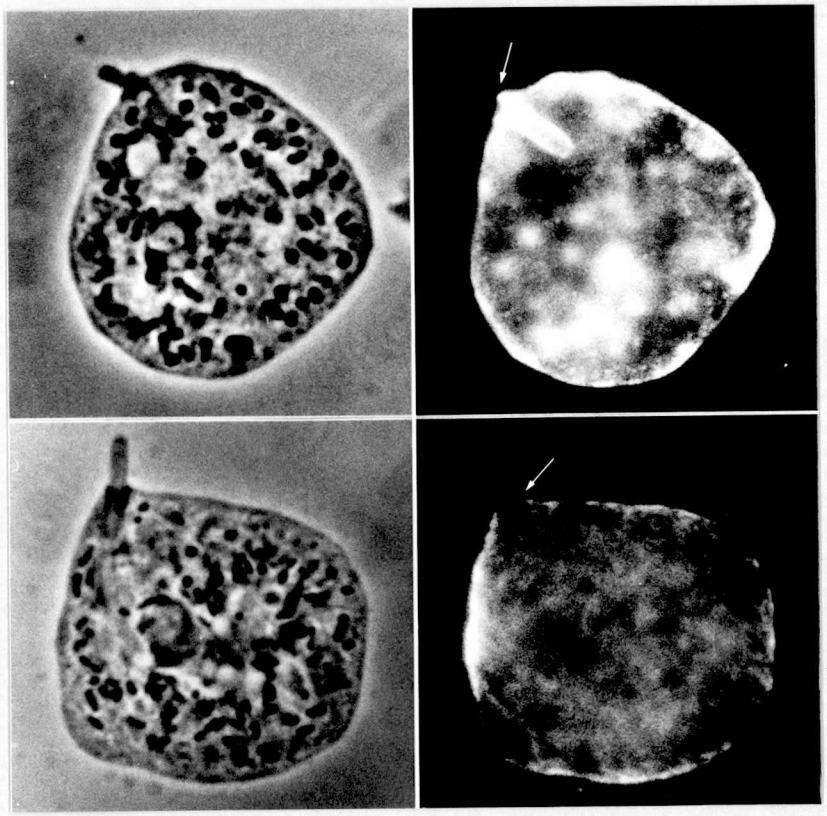

Fig. 19. Distribution of actin and myosin in phagocytotic apparatus in vegetative cells. Very specific actin staining (above) but no myosin staining (bottom) were seen around the ingected E. coli.

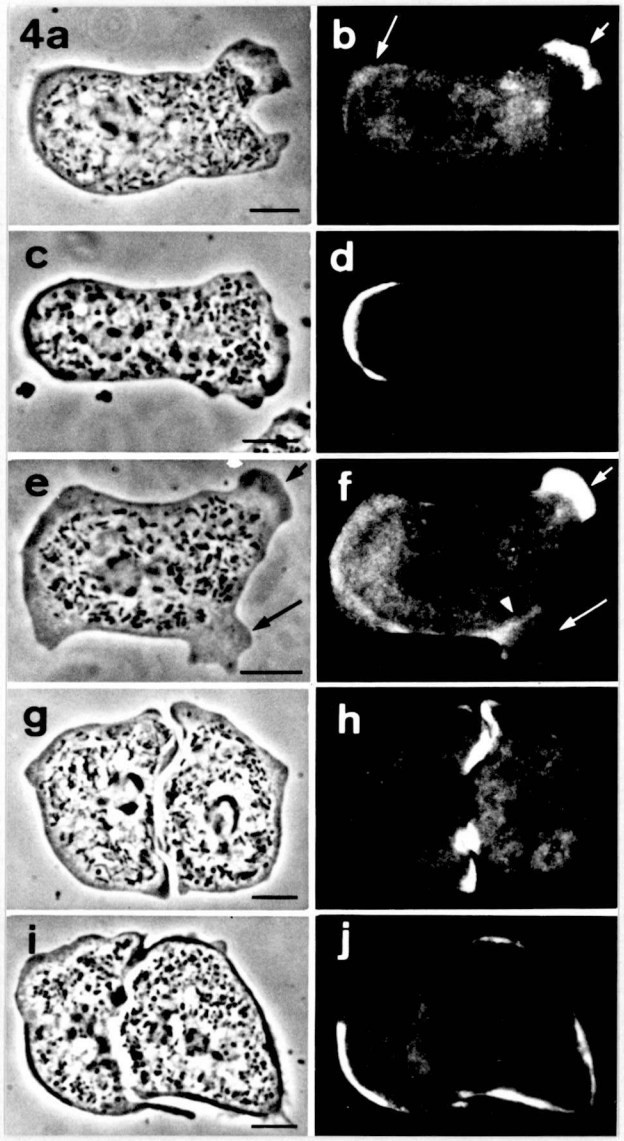

Fig.20. Distribution of actin and myosin in locomotory amoebae prepared by the agar-overlay technique. (a, b) An actively locomoting cell stained with anti-actin. Note the bright staining of the anterior pseudopode (short arrow). Staining of the posterior cortex (long arrow) was also prominent. (c, d) A monopodial cell stained with monoclonal anti-myosin (DM-2). The cortex in the posterior end was specifically stained. (e,f) A cell with actively extending pseudopode stained with anti-actin. The dark pseudopode (short arrow) was stained brightly whereas the light pseudopode (long arrow) was not. Note the staining at the boundary of the light pseudopode and the ground cytoplasm (arrow head). (g, h) Two cells in contact with each other stained with anti-actin. Bright staining was prominent in the contact regions. (i, e) Two cells in contact with each other stained with DM-2. The cortices on the other side of the contact regions were stained. Bar, 5 μm.

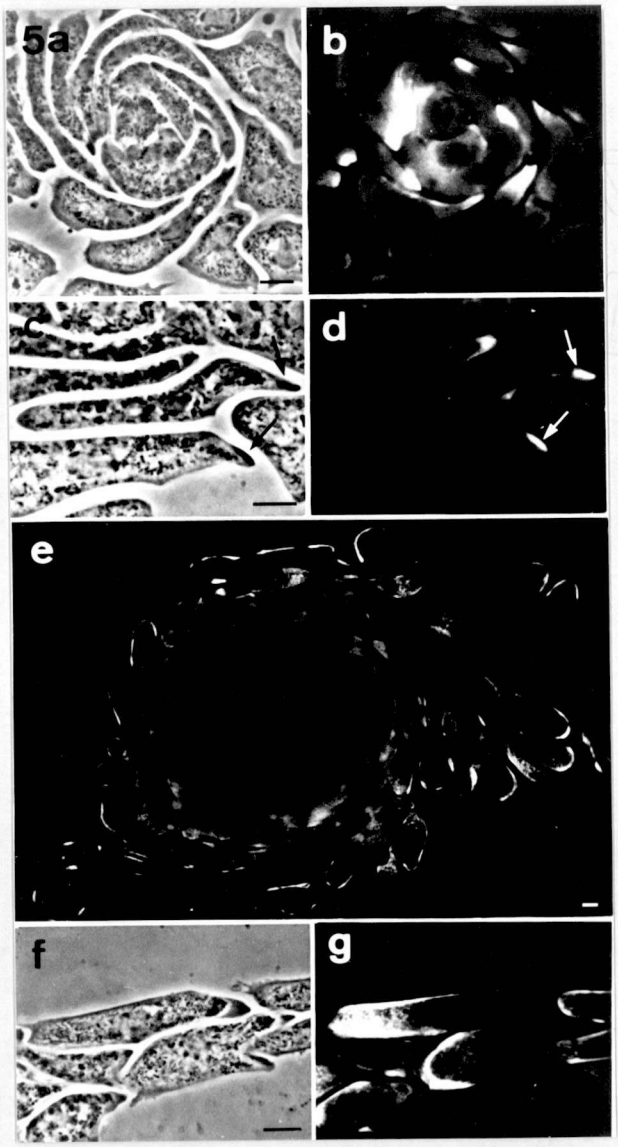

Fig. 21. Distribution of actin and myosin in aggregating amoebae prepared by the agar-overlay technique. (a, b) Staining with anti-actin of cell undergoing spiral movement to the aggregation center. The anterior pseudopode and the cell cortex were stained. (c, d) High magnification micrograhs of cells in the aggregation stream stained with anti-actin. Note the rod-like staining in the anterior pseudopode and a comparative phase-contrast image (arrows). (e) Macroscopic immunofluorescence of the aggregation center stained with monoclonal anti-myosin (DM-2). Staining of the lateral as well as the posterior cortex was prominent in the cells at the outermost periphery of the aggregate. (f, g) High magnification micrographs of cells in the aggregation stream stained with DM-2. Note the specific staining of the lateral as well as the posterior cortex. Bar, 5 μm.

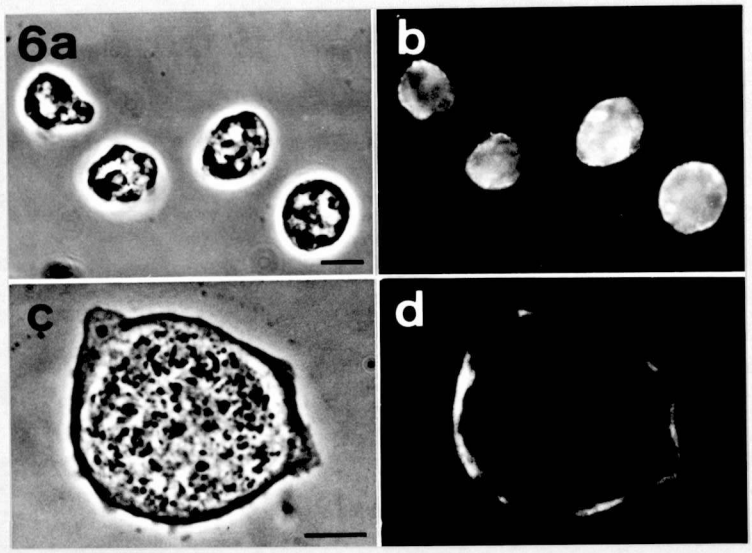

Fig. 22. (a, b) Immunofluorescence of suspended cells prepared by a conventional method. The cells were fixed with formaldehyde, extracted with methanol, then stained with anti-actin. The cell periphery was stained mostly brightly, showing the plausiblility of cortical staining after the agar-overlay procedure (see Discussion). (c, d) Immunofluorescence using polyclonal anti-myosin serum, showing the staining pattern was essentially identical to that with DM-2(see Discussion). Bar, 5 μm.

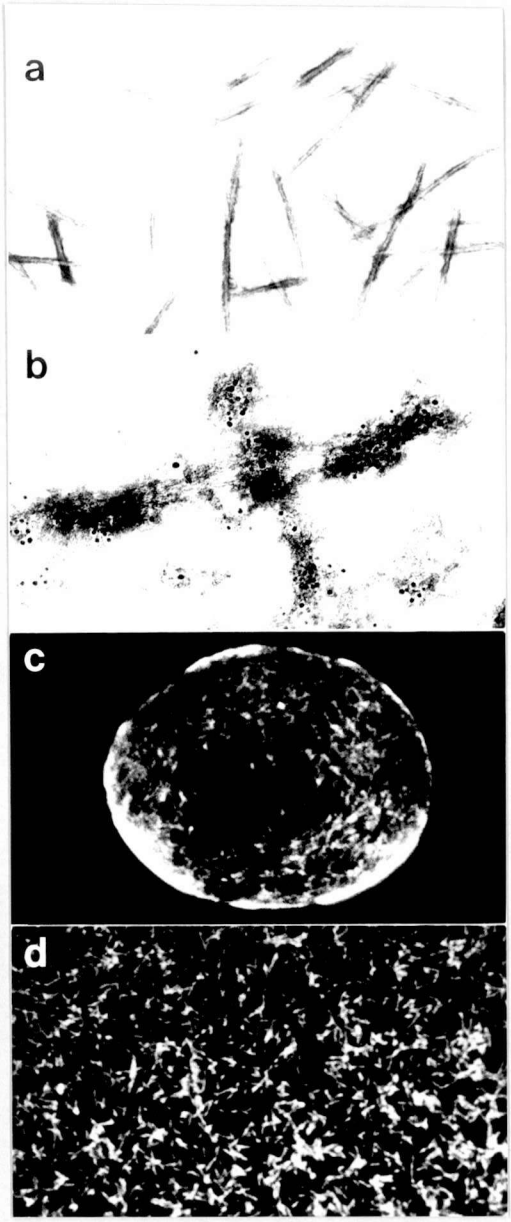

Fig. 23. Electron microscopic and immunofluorescence micrographs of reconstituted thick filaments of Dictyostelium myosin, and in situ localization of the presumptive thick filaments as shown by agar-overlay immunofluorescence. (a) Negative staining of reconstituted thick filaments (x 30,600). (b) Immunogold staining of purified myosin thick filaments (x122,400). Reconstituted thick filaments were placed on a poly-L-lysine-coated grid, incubated with DM-2 antibody, and stained with colloidal gold-conjugated second antibody. The monoclonal anti-Dictyostelium myosin is bound to the reconstituted thick filaments. (c) Immunofluorescence micrograph of Dictyostelium cell prepared by agar-overlay immunofluorescence (x 1,800). Rod-like fluorescent shapes (0.1-0.2 μm wide, 0.7 μm long) were visible. (d) Immunofluorescent staining of purified myosin thick filaments (x 1,800). Reconstituted thick filaments were placed on a poly-L-lysine-coated cover slip, incubated with DM-2 antibody, and stained with FITC-labeled second antibody.

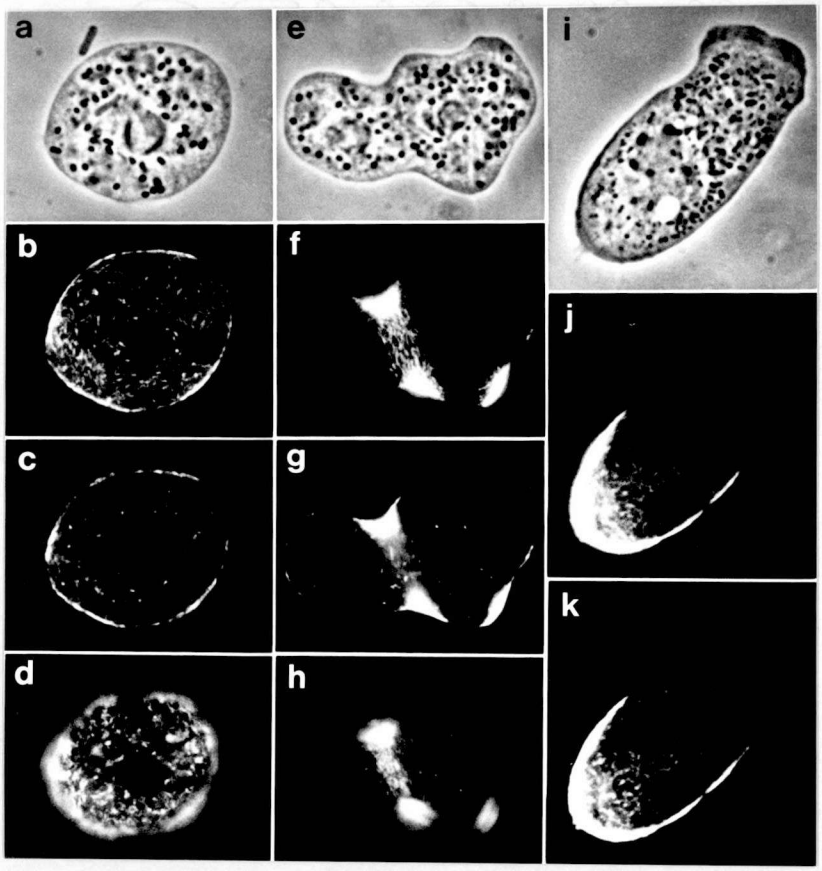

Fig. 24. Specific distribution of myosin rods in Dictyostelium amoebae. (a-d) Phase-contrast (a) and fluorescence (b-d) micrographs showing specific localization of myosin rods at the cortical region of a vegetative cell (x 1,340). Immunofluorescence micrographs taken at three different focal planes of the cell verified that the rods were localized only at the upper (b) and lower (d) cortices. Note that the rods are aligned in parallel with the cortex. (e-h) Phase-contrast (e) and fluorescence (f-h) micrographs showing the distribution of myosin rods aligned in parallel forming a contractile ring-like array (x1,230). The micrographs taken at the upper (f), middle (g), or lower (h) plane clarified that the rods were arranged in a peripheral, circular ring at the cleavage furrow. (i-k) Phase-contrast (i) immunofluorescence (j, k) micrographs showing that the myosin rods were specifically localized in the posterior cortex of a polarized cell and formed linear alignments. (j, k) Immuno-fluorescence micrographs taken at the upper (j) or middle (k) plane demonstrated that the rods were localized in the endoplasm (k) as well as in the cortex (j) at this stage (x 1,340).

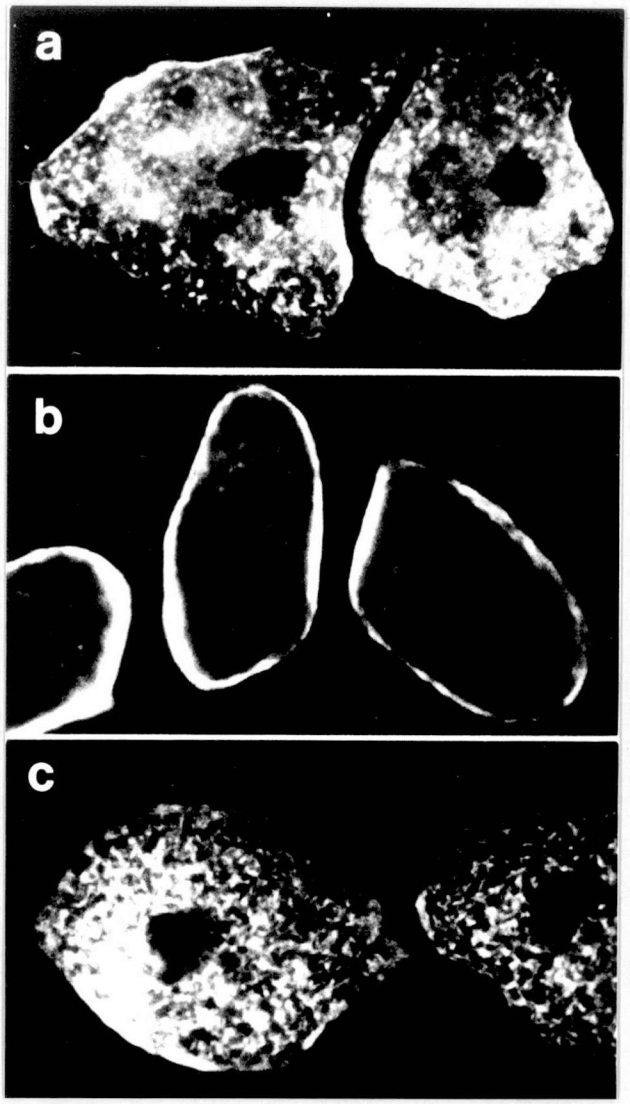

Fig. 25. Changes in the distribution of myosin rods in response to exogenously added cAMP. 10^{-6} M cAMP solution in phosphate buffer was added to aggregation-competent cells overlaid with a thin agarose sheet at 5 °C. After indicated time, the cells were plunged into -15 °C methanol containing 1% formalin and prepared for the agar-overlay immunofluorescence. (a) Control cell. (b) 2 min, and (c) 3 min after cAMP application (x 1,825). Note the disappearance of the endoplasmic rods and their accumulation at the cortex in (b), and their reappearance in (c).

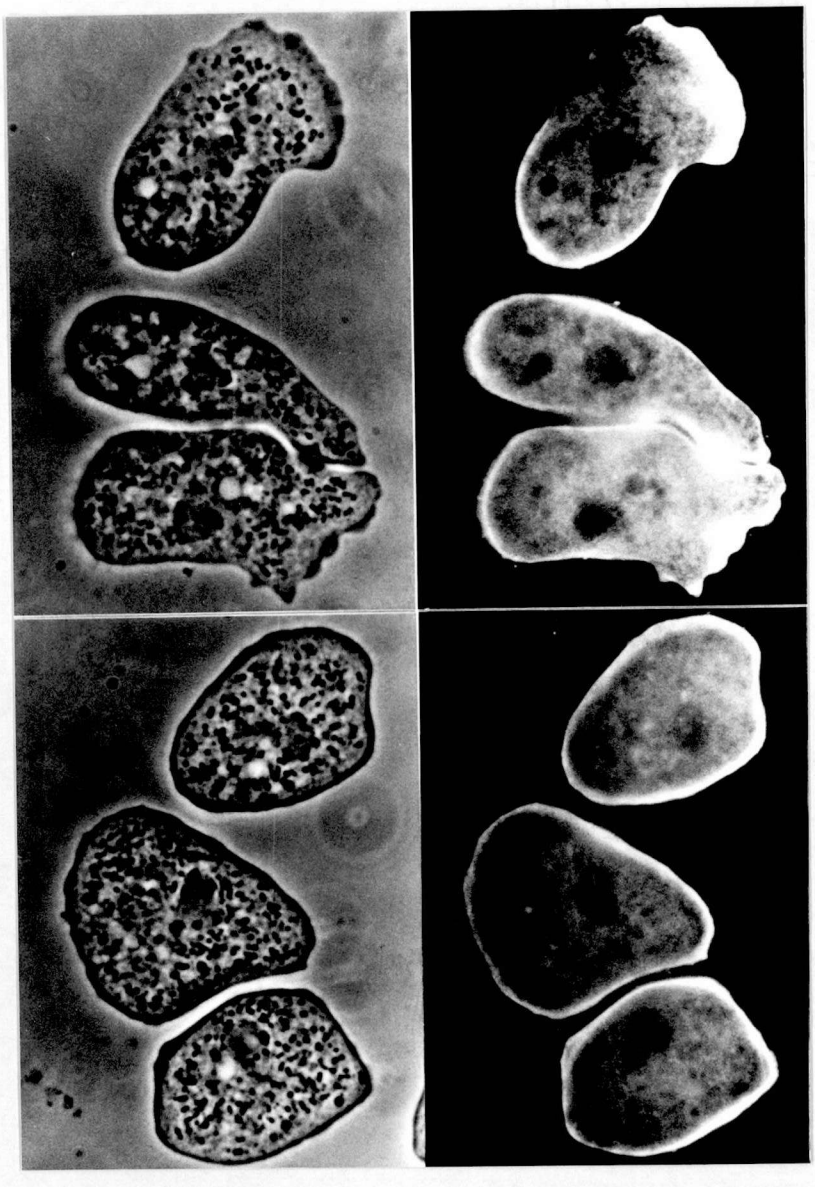

Fig. 26. Distribution of actin in responding cells to cAMP. 10^{-6} cAMP was added to aggregation-competent cells. After 2 min, cells were fixed and prepared for indirect immunofluorescence using anti-actin. Actin staining in untreated cells (above) were localized at pseudopode, contact region and tail cortex, but in responding cells, uniformly localized at the cortex.

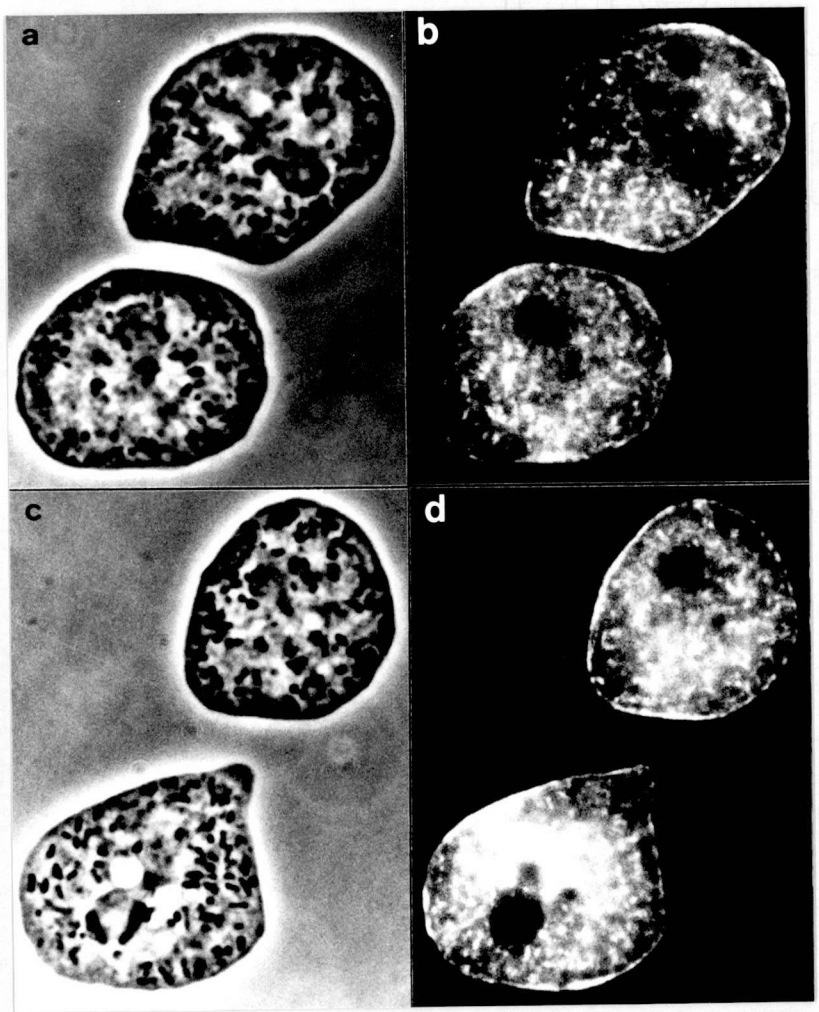

Fig. 27. Changes in distribution of myosin rods in vegetative cells responding to folic acid and cAMP. After 3 min of the application of folic acid (above) or cAMP (bottom) on vegetative cells, myosin rods appeared in the endoplasm. In one more min, these rods disappeared from the endoplasm and relocalized at the cortex.

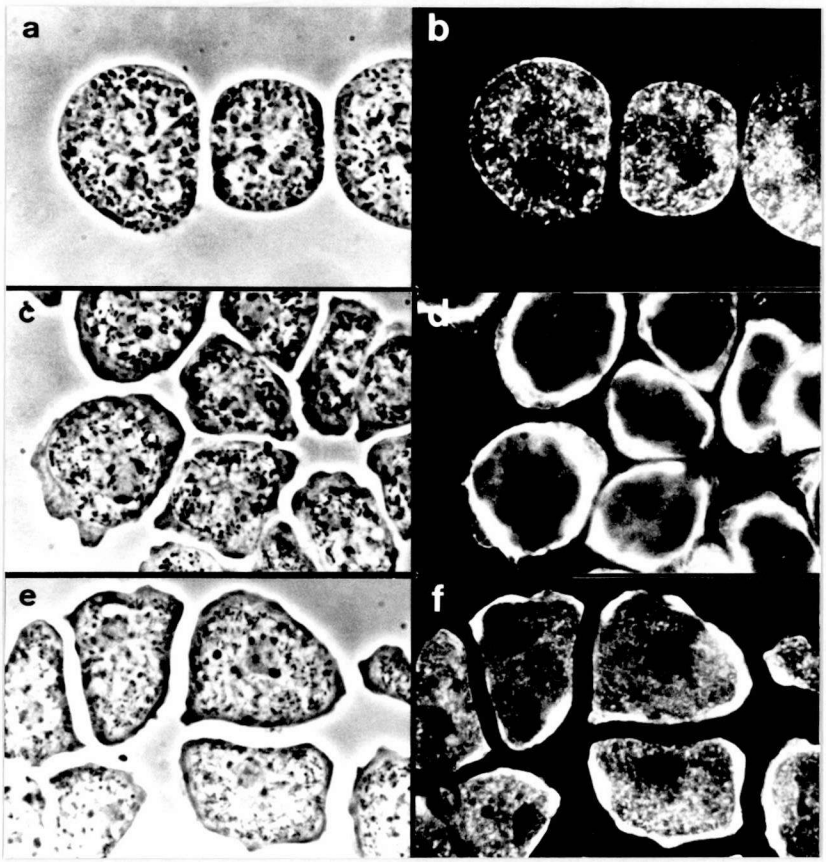

Fig. 28. Changes in distribution of myosin rods in vegetative cells and aggregation-competent cells treated with calcium ionophore A23187. Ionophore induced the reversible changes in distribution of myosin rods in vegetative cells (a,b) and aggregation-competent cells (c,d). The treatment with ionophore for 3 min resulted in same changes in distribution of myosin rods as chemoattractants. However, calcium ionophore could not induce such changes in the absence of extracellular calcium (e,f).

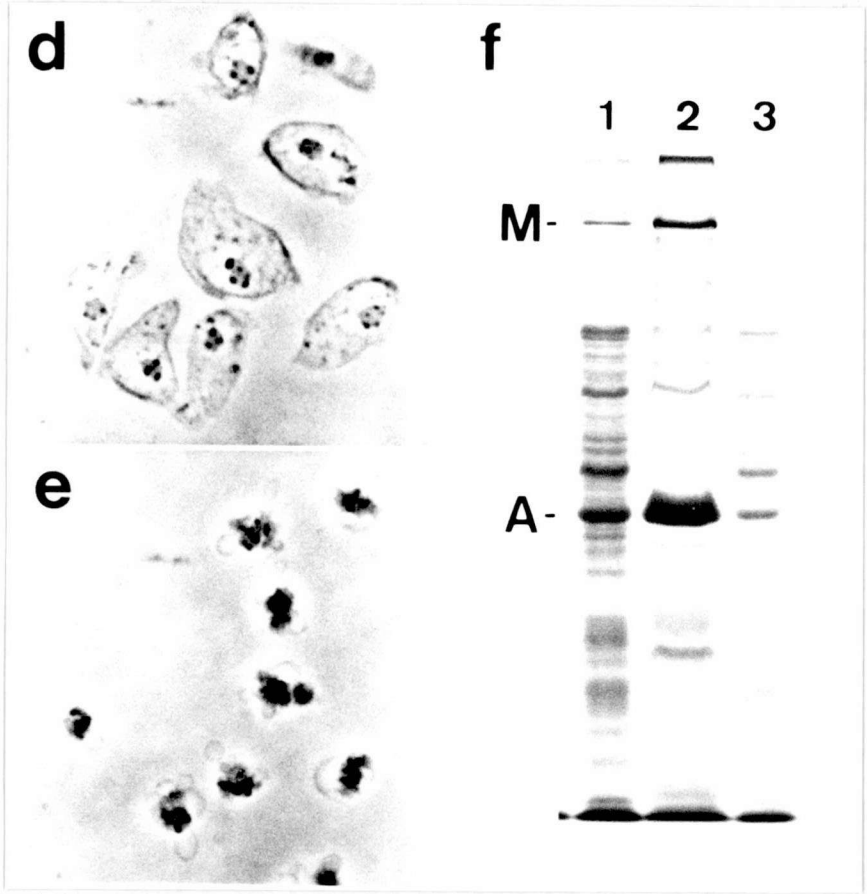

Fig. 29. The contractility of Triton-insolubule ghosts of Dictyostelium. Cells in aggregation phase were overlaid with a thin agarose sheet and treated with 10^{-6} M cAMP at 5°C. After 2 min, when the endoplasmic rods disappeared as shown in Fig.25, the cells were permeabilized with P-buffer containing 0.5% Triton X-100 for 10 min at 0°C, then extracted with the P-buffer for 5 min. A phase-contrast micrograph (d) showed that the Triton-insoluble ghosts contained the cell cortex, nucleus and some cytoplasmic debris. The ghosts contracted in a few seconds after application of the P-buffer containing 1 mM ATP (d, e). SDS PAGE showed that actin and myosin comprised 25% and 50% of the cellular protein, respectively, in the Triton-insoluble ghosts. Lane 1, whole cell lyaste (100 μg); lane 2, Triton-insoluble proteins (85 μg); lane 3, Triton-soluble proteins (50 μg). A, actin; M, myosin heavy chain.

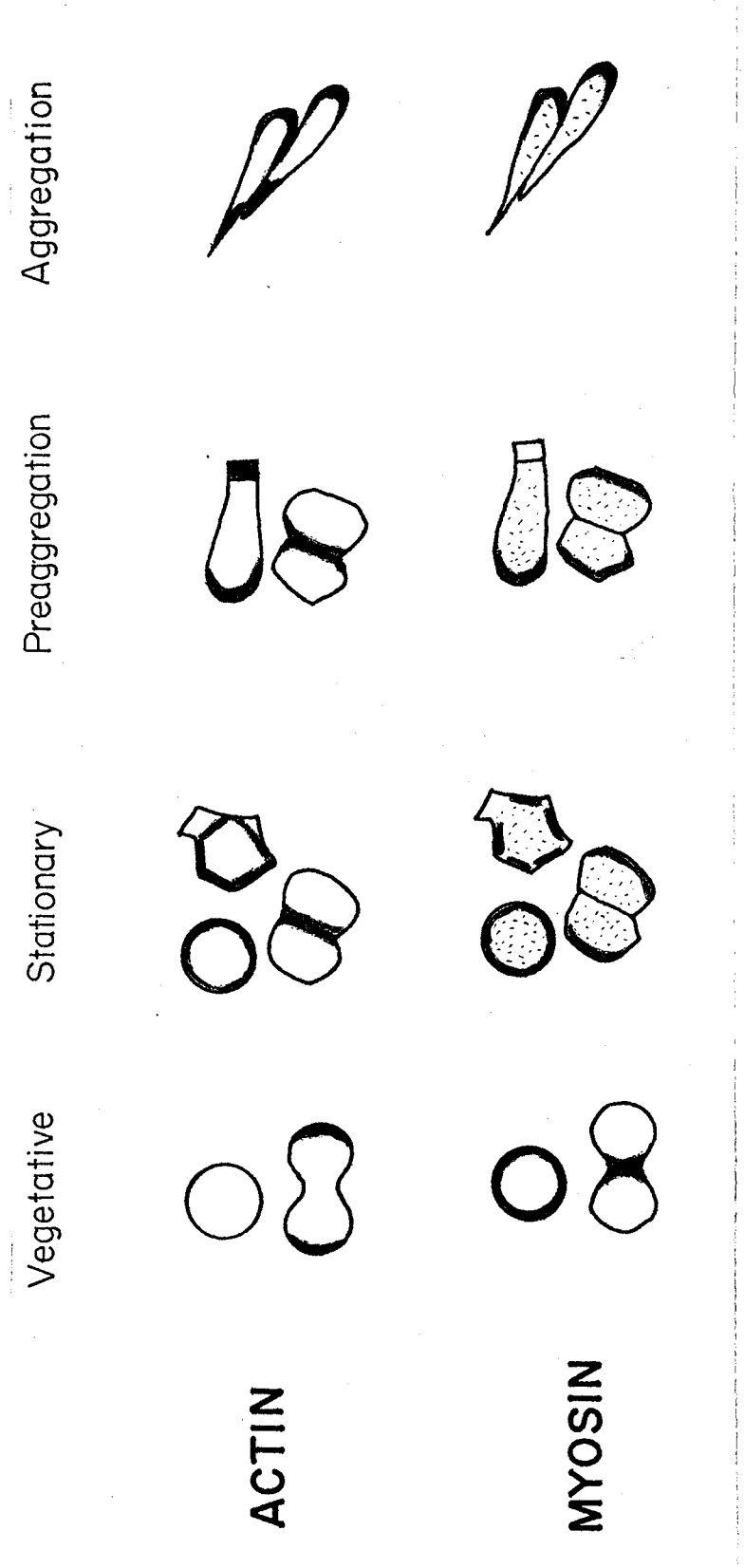

Fig. 30. The shematic distributions of actin and myosin in Dictyostelium amoebae during early development.

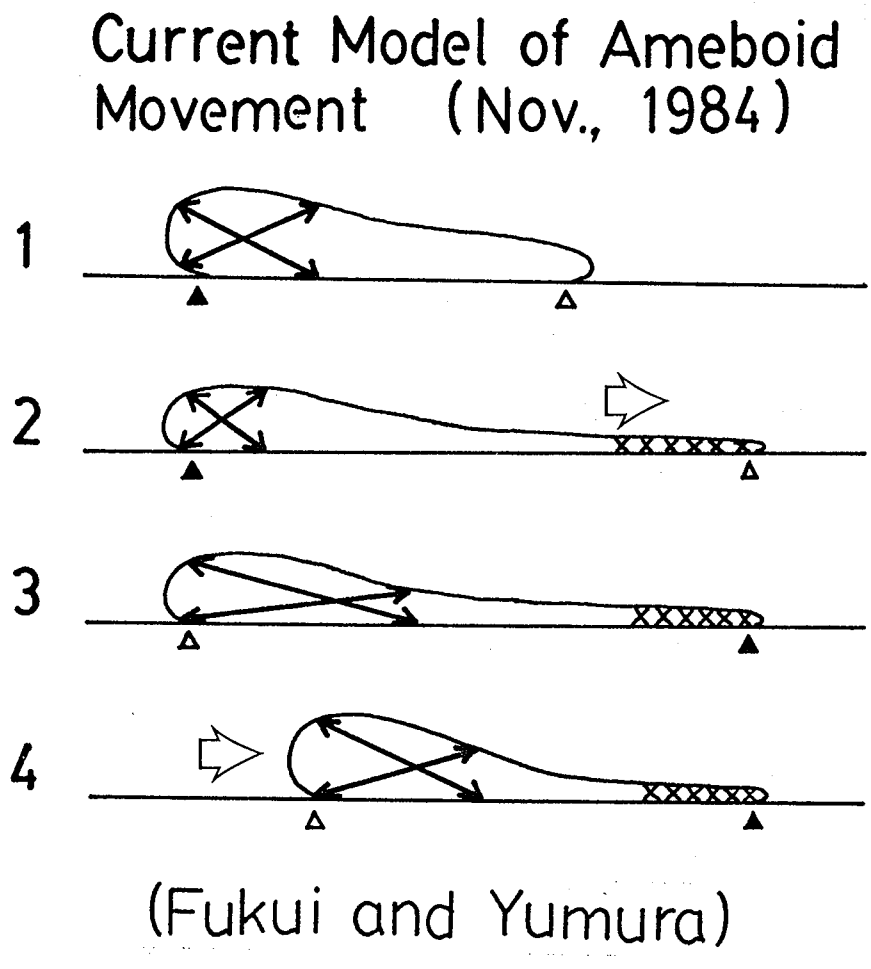

Fig. 31. Current model of amoeboid movement in Dictyostelium. Sequential steps in locomotion of a cell on the substratum are drawn. (1) A possible attachment site (filled triangle) at the tail and a loose attachment site (open triangle) at the front on the substratum are shown. Two crossed double arrows show the state of contraction of a tail cortex of the cell. (2) The contraction of the tail cortex induces the extention of a pseudopode containing dense meshwork of actin filaments (cross-stitch at the front) toward the right (broad arrow). (3) A tight attachment site is produced at the front region and the tail attachment site is loosened, accompanying with the relaxation of a tail cortex. (4) The tail is pulled forward (broad arrow) resulting in the progression of a cell body.

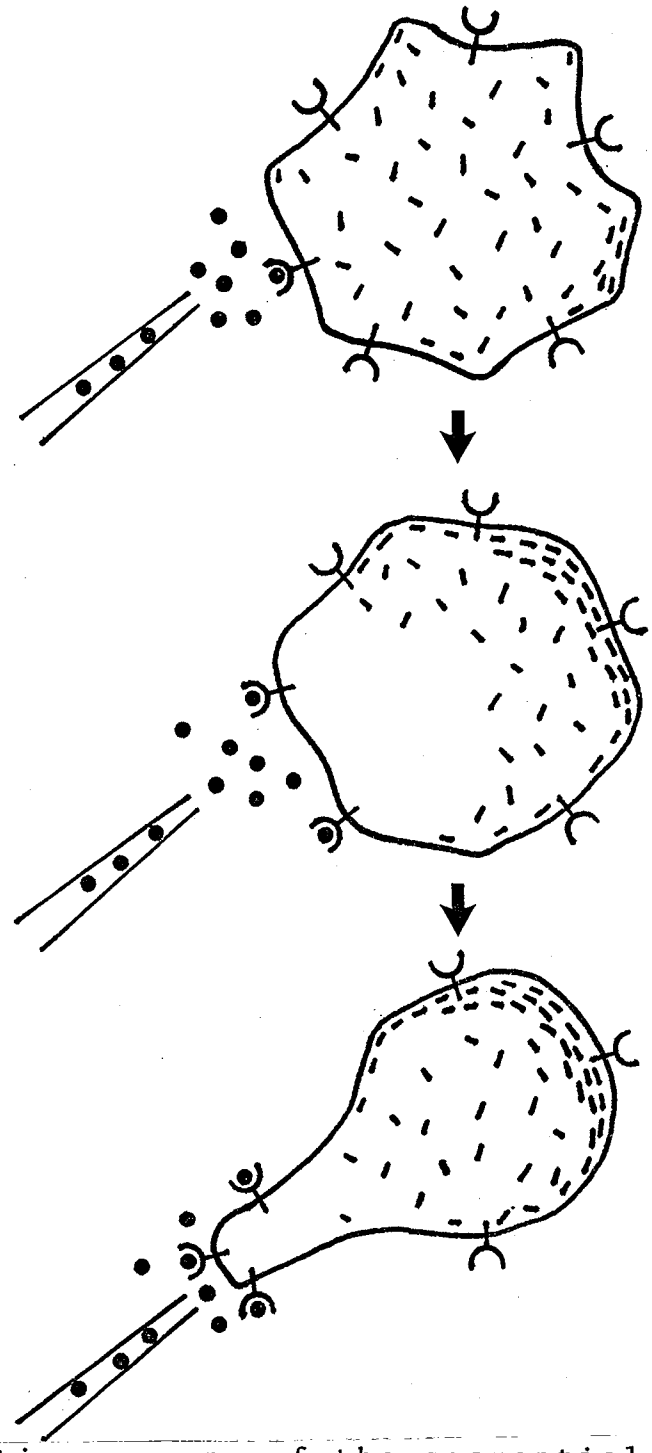

Fig. 32. Diagramatic summary of the sequential steps in extention of a pseudopode in response to chemoattractant. (above) In a round aggregation-competent cell, myosin rods are uniformly distributed in endoplasm as well as at the cortex. Receptors of chemoattractants are uniformly distributed on the cell membrane, too. (middle) When chemoattractants in a microcapillary is applied to the local region of the cell, chemoattractants bind to receptors on local part of cell membrane near the capillary. The binding of chemoattractats on the receptors induces the local disappearance of myosin rods and the accumulation at the cortex on the opposite side of the microcapillary. (bottom) The cortex on the opposite side of the microcapillary contracts and endoplasm is pushed forward to the microcapillary, resulting in the resumption of myosin rods in distribution and the extention of a pseudopode.

Table 1. Effects of chemical fixations on the disruption of in situ myosin rods of Dictyostelium

Glutaraldehyde*1)	OsO_4*2)	Myosin rods*3)
0%	0%	+
1	0	±a)
2	0	−
0	0.01	+
0	0.1	±b)
1	0.01	−
2	0.1	−

*1) Stock solution of glutaraldehyde (25%; Electron Microscopy Science) was diluted with PBS (138 mM NaCl, 2.7 mM KCl, 8 mM phosphate buffer, pH 7.2). The sample was fixed for 30 min at 25°C.

*2) Stock solution of OsO_4 (8%; Merck) was diluted with PBS. The sample was fixed for 10 min at 4°C.

*3) The degree of the fluorescent staining of the rods was judged according to the criteria as shown below:

−: no specific rod-like fluorescence was detactable, partially because of the autofluorescence caused by glutaraldehyde.

±a): faint rod-like fluorescence was identified in the bright autofluorescence.

±b): dotted fluorescence was seen instead of the rod-like fluorescence.

+: apparently normal rod-like fluorescence

Table 1. Aggregation-competent cells were first subjected to agar-overlay immunofluorescence, then to fixation with glutaraldehyde and/or osmium tetraoxide (OsO_4). The in situ thick filaments were suspectible to chemical fixation and were totally disrupted by the fixation with 0.1% OsO_4 for 10 min at 4 °C.